UNIVERSIDADE DE LISBOA
FACULDADE DE CIÊNCIAS
DEPARTAMENTO DE ENGENHARIA GEOGRÁFICA, GEOFÍSICA E ENERGIA

Paleo- and rock magnetism of the Central Atlantic Magmatic Province (CAMP) from Portugal: global-scale correlations and implications for the paleogeography of Iberia at 200 Ma.

Susana de Lurdes Alves Fernandes

Dissertação

Mestrado em Ciências Geofísicas

Especialização em Geofísica Interna

2013

UNIVERSIDADE DE LISBOA

FACULDADE DE CIÊNCIAS

DEPARTAMENTO DE ENGENHARIA GEOGRÁFICA, GEOFÍSICA E ENERGIA

Paleo- and rock magnetism of the Central Atlantic Magmatic Province (CAMP) from Portugal: global-scale correlations and implications for the paleogeography of Iberia at 200 Ma.

Susana de Lurdes Alves Fernandes

Dissertação

Mestrado em Ciências Geofísicas

Especialização em Geofísica Interna

Dissertação orientada pelo Prof. Doutor Eric Font do IDL-UL

2013

Acknowledgments

I would firstly like to thank Línia Martins for guidance and assistance with the thin sections from Algarve outcrops and to Claire Carvalho for hysteresis and FORC measurements.

A special thank to Eric Font, Marta Neres and Pedro Silva for always being available to clarify questions related to this work.

And finally, a special thank to my colleagues: Jorge Ponte and Ana Lopes for the support shown whenever was necessary and, obviously, to my friends, family and boyfriend for the patience and willingness to help.

"*Agir, eis a inteligência verdadeira. Serei o que quiser. Mas tenho que querer o que for. O êxito está em ter êxito, e não em ter condições de êxito. Condições de palácio tem qualquer terra larga, mas onde estará o palácio se não o fizerem ali?*"

Fernando Pessoa

Abstract

The Central Atlantic Magmatic Province (CAMP) is one of the largest igneous provinces of the Phanerozoic and is believed to be coeval with the biological crisis of the Triassic-Jurassic boundary (~200Ma). These lavas have been extensively studied in the United States and Morocco, however little attention has been given to the CAMP lavas from the south of Portugal for which geochemical data have been recently published. Paleomagnetic methods can play a key role in the paleogeographic reconstruction of CAMP lavas at a global scale, and also be useful for geochronological purposes. Here I present a detailed rock- and paleo-magnetic study of the Portuguese CAMP lavas from the Algarve basin's outcrops. It is showed that, despite severe superficial alteration, rocks preserved their primary magnetic mineralogy represented by an assemblage of fine titanomagnetite as the dominant carriers of the NRM. After cleaning by alternating field, a characteristic remanent magnetization (ChRM) is isolated at Dec=353.4º, Inc=52.8º (a95=1.5º, N=257) and Dec=0º, Inc=50.4º (a95=8.3º, N=8) for sample and site-based mean respectively. The results yielded a statistically well-defined pole at: Plat=83.3º and Plong=236.1º (A95=1.8º) and Plat=84.4º and Plong=177.9º (A95=9.8º) for sample and site-based paleomagnetic pole, respectively. Position of the corresponding paleomagnetic pole is significantly different from the referenced Messejana dyke's pole. This discrepancy is due to the presence of two VGP's. One of the VGP's group (component A) falls within the Messejana VGP's distributions whereas the other has no equivalent with other younger pole. We show the enigmatic direction of component B is not product of remagnetization, lightning or difference in age. We suggest significant tectonic movements in the Algarve's basin as a potential cause. On a magnetostratigraphic point of view, all lavas carry a normal (positive) magnetization confirming the previous results that demonstrated the absence of the well-known E23r reverse anomaly in Morocco. VGP's directions per flow vary slightly within the lava pile suggesting rapid eruptions.

Key-Words: CAMP, lavas, paleomagnetism, magnetic mineralogy, Iberia.

Resumo expandido

A Província Magmática do Atlântico Central (CAMP) é considerada uma das maiores províncias ígneas do Fanerozóico e é contemporânea da crise biológica que marca a transição Triássico-Jurássico (Tr-J) (~200 Ma). Vestígios desta província são encontrados em quatro continentes com uma área que excede os 100 milhões de km2, o que leva muitos cientistas a acreditar que a crise biológica que marca este período é provocada pela erupção desta província magmática. Neste sentido, as lavas da CAMP têm sido extensivamente estudadas, especialmente nos Estados Unidos e em Marrocos, não só para perceber o seu sincronismo com a crise biológica, mas também para estudos de paleoreconstituição usando métodos paleomagneticos.

Em Portugal as evidências da CAMP são representadas por um dique de cerca de 540 Km de extensão, o dique da Messejana, e por afloramentos de lavas continentais distribuídos ao longo das bacias do Algarve e de Santiago do Cacém. A importância do estudo destas lavas recai sobretudo na necessidade de calcular novos polos paleomagneticos para reconstituir a paleogeografia da placa Ibérica à 200 Ma, que ainda hoje é um assunto discutido. O problema principal destas reconstituições paleogeográficas reside na escassez de dados paleomagneticos de qualidade. De facto, o único polo paleomagnetico para a Ibéria à 200 Ma é o polo da Messejana que servirá de referência para o presente estudo.

A descoberta da anomalia E23r imediatamente abaixo do limite Triássico-Jurássico na bacia de Newark, Estados Unidos, e posteriormente sugerido nas lavas da CAMP em Marrocos, tem sido também um assunto bastante debatido uma vez que a presença desta anomalia nas lavas da CAMP é usada como marcador temporal. Em Newark, esta anomalia encontra-se abaixo do limite Tr-J e das lavas da CAMP. Em Marrocos, foi sugerida a presença desta anomalia E23r no meio da sequência basáltica levando à conclusão que a CAMP em Marrocos é mais antiga que em Newark e anterior ao limite Tr-J. Porém, os resultados que foram adquiridos no meu projecto de licenciatura demonstraram que a inversão geomagnética encontrada nas lavas em Marrocos era na realidade um artefacto resultante de uma remagnetização química. A eventual presença de anomalias inversas nos basaltos precisa de ser verificada em Portugal.

O propósito principal deste trabalho é i) obter um novo polo paleomagnetico para a placa Ibérica aos 200 Ma e ii) verificar a presença da anomalia E23r em Portugal. Devido à forte alteração química que afecta a maioria dos afloramentos da região do Algarve, um estudo preliminar da mineralogia magnética torna-se indispensável.

A amostragem de campo consistiu em três excursões de cinco dias cada, financiadas pelo projecto FCT (IMPACTO; ref. PTDC/CTE-GIX/117298/2010). Mais de 300 amostras foram recolhidas desde a extremidade oeste da bacia do Algarve até à fronteira com Espanha. Foram privilegiados sítios de amostragem onde dados geoquímicos foram recentemente publicados.

A parte experimental do trabalho foi dividida em duas partes: 1. Magnetismo de rocha e 2. Paleomagnetismo. O magnetismo de rocha permite a identificação do tipo, natureza e tamanho de grãos dos minerais portadores da magnetização natural remanescente da rocha. Para isto, os principais métodos usados foram: Magnetização remanescente isotérmica (IRM) que informa sobre a coercividade dos minerais ferromagnéticos presentes na amostra; Curvas termomagnéticas que identificam os minerais magnéticos presentes a partir da determinação da temperatura de Curie (Néel); Day-Plot e FORC's usados na identificação do tamanho de grão e coercividade dos principais portadores magnéticos.

A secção do Paleomagnetismo, baseou se essencialmente na desmagnetização usando campo alternado para calcular as direcções das componentes magnéticas presentes nas rochas. As componentes magnéticas são calculadas com base no método de análise das componentes principais (ACP) usando a estatística de Fisher que controla a qualidade das componentes calculadas. Posteriormente, o polo paleomagnetico calculado é qualitativamente avaliado usando o factor Q dos critérios de Van Der Voo.

Os resultados mostram que apesar da forte oxidação que afecta a maioria das amostras da bacia do Algarve a magnetização remanescente é estável e é essencialmente portada por titanomagnetites. Estes resultados são inferidos pela análise de curvas termomagnéticas que a baixas temperaturas mostram a característica transição de Verwey (~-160ºC) da magnetite e a altas temperaturas apresentam

temperaturas de Curie típicas da titanomagnetite (entre 200ºC e 560ºC). A análise das IRM usando o tratamento de Kruiver revela que para a maioria das amostras existe para além da magnetite, um mineral mais coercivo que não é identificado nas curvas termomagnéticas. Este mineral mais coercivo existe em pequena proporção nas amostras e pensa-se ser hematite, mineral comum nos basaltos. Nas curvas termomagnéticas, um outro mineral é identificado aos ~250ºC-350ºC. Este mineral é interpretado como sendo maghemite, a fase oxidada da magnetite. A associação titanomagnetite, maghemite e hematite corresponde à mineralogia clássica de basaltos continentais com algum grau de oxidação.

As amostras submetidas à desmagnetização em campo alternado (AF) mostram padrões de desmagnetização bastante estáveis, todas elas com polarização normal (positiva) e em geral com distribuições bem agrupadas por sítio nos estereogramas. Duas componentes foram isoladas: i) uma componente magnética eliminada com campos inferiores a 20 mT e interpretada como sendo uma componente viscosa, adquirida em campo fraco posteriormente à formação da rocha; ii) Uma componente magnética estável em campos elevados (> 40 mT) com uma direcção N-NE e inclinação positiva.

Das 280 amostras analisadas, 257 foram usadas para calcular a componente média das amostras, o que representa uma percentagem de sucesso ~92%. Os "outliers" foram eliminados usando o método de Vandamme 1994. A componente magnética média calculada para todas as amostras, corrigidas pelo acamamento (contacto com sedimentos abaixo das camadas de lavas ou as paredes das escoadas) é: Dec=353.4º, Inc=52.8º (a95=1.5º, N=257). Também é possível fazer se uma média da componente média por sítio paleomagnético. E nesse caso, para oito sítios tem-se: Dec=0º, Inc=50.4º (a95=8.3º, N=8). A componente magnética média é posteriormente usada para calcular o polo paleomagnetico e a sua confiabilidade é avaliada estatisticamente pelos parâmetros de Fisher nomeadamente: k, o parâmetro de dispersão das amostras em relação a uma dada população; a95, o intervalo de 95% de confiança na direcção magnética média; R, a direcção do vector resultante. Este parâmetro é relativamente importante devido à sua independência em relação ao número de amostragem, N. A componente média para todas as amostras e a componente média por sítio paleomagnético é: Plat=83.3º,Plong=236.1º, (A95=1.8º, K=25.9) e Plat=84.4º,Plong=177.9º, (A95=9.8º, K=32.9), respectivamente. Quando comparamos os polos obtidos com a curva de deriva polar da Ibéria, construída a partir de uma compilação de vários autores, não existe similaridade com o polo da Messejana ou com polos de idades mais recentes. Porém, se apenas considerarmos os polos geomagnéticos virtuais (VGP) de cada sítio de amostragem, observamos a presença de dois grupos de direcções distintas: um grupo (designado por componente A) com uma direcção média muito próxima do polo da Messejana e um outro grupo (designado por componente B) com uma direcção média muito distinta do polo da Messejana e sem qualquer similaridade com polos de idade mais recente da APWP da Ibéria. Tendo em conta que a direcção da componente B é partilhada por 4 VGP's que estão todos localizados na parte central da bacia do Algarve, sugerimos que essa direcção da componente B pode ser o resultado de movimentos tectónicos posteriores.

Esses resultados fornecem uma base sólida para estudos paleomagneticos futuros nas lavas da CAMP em Portugal. Uma perspectiva futura é estudar novos sítios paleomagneticos de outra bacia, nomeadamente a bacia de Santiago do Cacém, para verificar a origem da componente B e para obter um novo polo paleomagnético com critérios estatísticos satisfatórios.

Palavras-chave: CAMP, Paleomagnetismo, Magnetismo de Rocha, Polo magnético

Index

Figure Index

Table Index

List of acronyms

%	Percentage
µm	micrometer
A40	Alteration index
a95	95% confidence level on the mean direction (Fisher distribution)
A95	95% confidence level of the direction of the paleomagnetic pole
A/m	Ampere per meter
AA	Atalaia (Paleomagnetic site)
AL	Alte (Paleomagnetic site)
AY	Ayamonte (Paleomagnetic site)
AF	Alternating field
Ar	Argon
APWP	Apparent Polar Wander Path
$B_{1/2}$	Mean coercivity force
CAMP	Central Atlantic Magmatic Province
ChRM	Characteristic Remanent Magnetization
CLG	Cumulative Log-Gaussian
Dec	Declination
DP	Dispersion parameter (Kruiver treatment)
e.g.	For example
FORC	First Order Remanence Curve
FP	Caminho velho para Alte (Paleomagnetic site)
GAP	Gradient Acquisition Plot
GPTS	Global Polarity Time Scale
H_a	Reversal magnetic field
H_b	Saturating magnetic field
H_{cr}	Field needed to reduce M_{rs} to zero
H_c	Bulk coercivity
HT	Hortas do Tabual (Paleomagnetic site)
*HT	High temperature (measurement)
H_u	Interacting field
i.e.	Namely
Inc	Inclination
IRM	Isothermal Remanent Magnetization
JG	Jardins do Guadiana (Paleomagnetic site)
k	Precision parameter of ChRM (Fisher distribution)
K	Precision parameter of the paleopole
Kdf	frequency dependent susceptibility

Khf	high field frequency susceptibility
Klf	low field frequency susceptibility
Km	Kilometer
kyr	Thousand years
LAP	Linear Acquisition Plot
Lat	Latitude
LIP	Large Igneous Province
Long	Longitude
LT	Low Temperature (measurement)
m	meter
Ma	Million years
MD	Multi-domain
M_{rs}	Maximum Saturation Remanence (Hysteresis parameter)
M_s	Maximum Saturation Magnetization (Hysteresis parameter)
mT	mili Tesla
N	Number of samples
NRM	Natural Remanent Magnetization
Plat	Latitude of the paleomagnetic pole
Paleolat	Paleolatitude of the paleomagnetic pole
Plong	Longitude of the paleomagnetic pole
PSD	Pseudo- Single- Domain
PSV	Paleo Secular Variation
QO	Quinta da Ombria (Paleomagnetic site)
R	Intensity of the resultant vector (Fisher distribution)
RL	Ribeira de Alte (Paleomagnetic site)
SAP	Probability Acquisition Plot
SB	São Bartolomeu (Paleomagnetic site)
SiO_2	Silica content
SIRM	Saturation Isothermal Remanent Magnetization
SD	Single domain
SMQF	São-Marcos Quarteira Fault
SP	Superparamagnetic
VGP	Virtual Geomagnetic Pole
VRM	Viscous Remanent Magnetization
T	Tesla
TiO_2	Titanium oxide
Ti	Titanium
Tr-J	Triassic- Jurassic

1. Introduction

The Central Atlantic Magmatic Province (CAMP) is one of the largest Phanerozoic continental Large Igneous Province (LIP), associated with the disruption of Pangea and the opening of the central Atlantic Ocean (Marzoli et al., 1999). Similar to the Siberian and Deccan Traps, the CAMP magmatism is apparently coeval with one of the five most severe mass extinction in the Phanerozoic, the Triassic Jurassic (Tr-J) boundary ca. 200 Ma ago (McHone, 2002; Pálfy, 2003). Marzoli et al. (2004) suggested that the CAMP volcanism in Morocco preceded the Tr-J boundary, and thus can be responsible for the associated biotic crisis. Such hypothesis is based on the presence of short geomagnetic reversals recorded in the Moroccan CAMP lava (Knight et al. 2004) correlated by the authors to the E23r anomaly of the Newark basin, USA (Kent and Olsen, 1999). However, the primary origin of these magnetic reversals has been recently challenged by the results brought during my bachelor scientific project and published in Font et al. (2011). In this work the authors demonstrated that the negative polarities are actually the product of remagnetization and hydrothermal processes. The debate remains open.

Paleomagnetic techniques may be conducted on CAMP's outcrops not only to study its possible relation to the Tr-J biological crisis, but more importantly, to infer the position and kinematic evolution of the continental plates contemporaneous with the eruption of these major magmatic province (Osete et al., 2011; Martínez et al., 2012; Palencia-Ortas et al., 2006; Osete and Palencia-Ortas, 2006). Even though the evolution of major plates, since Pangea break-up, is well known and constrained (Besse and Courtillot, 2002; Torsvik et al., 2008) paleoreconstruction of micro plates such Iberia is still problematic (Osete et al., 2011; Palencia-Ortas, 2006, Vissers and Meijer 2012; Neres et al., 2012). Neres et al. (2012) made a rigorous selection of paleomagnetic poles for the Iberian plate from Cretaceous to Late Jurassic ages and concluded that the Iberian Apparent Polar Wander Path (APWP) is coincident with the Global APWP of Torsvik et al. (2008) for ages younger than 120 Ma, but fails toward older ages. The lack of reliable paleomagnetic poles and precise radiometric ages, as well as uncertainties about Euler poles deduced from marine magnetic anomalies may be the source of this misfit for the interval of interest (~200Ma). For example, the only reliable paleomagnetic pole for the Iberian plate at 200 Ma is the Messejana pole (Palencia-Ortas et al., 2006). Thus, new reliable paleomagnetic poles are needed.

The aim of this work is to conduct a new rock magnetic and paleomagnetic study on CAMP lava's from the Algarve basin in order to: i) verify if the magnetic mineralogy of these rock is suitable for paleomagnetic investigation, ii) to test for the presence of E23r anomaly and iii)provide a new paleomagnetic pole for Iberia at 200 Ma. To reach these objectives, approximately 300 samples were collected from nine sites distributed along an E-W transect from Sagres (western Portugal) to Ayamonte (Spain). Field trips consist in three excursions of five days, which has been funded by FCT (IMPACTO: ref. PTDC/CTE-GIX/117298/2010). Magnetic measurements were conducted at the Paleomagnetic laboratory of IDL (Lisbon). Results provided a stable remanent magnetization, probably contemporaneous with the cooling of the CAMP lavas. However, the newly founded pole is significantly different from the referenced Messejana pole due to the presence of two different and well-constrained VGP's distribution. One of the distributions, "A component", is close to the reference pole, but the other, "B component", is significantly different from the Messejana pole or any pole from the Iberian APWP. This misfit is interpreted as the result of significant pos-eruption tectonic movements. Finally, the results bring new insights to discuss the age and duration of CAMP volcanism in Portugal as well as its correlations with CAMP sections cropping out in Morocco and USA.

2. Geological settings and previous works

2.1 CAMP (Global distribution)

The Central Atlantic Magmatic Province (CAMP) is one of the largest flood basalt provinces known in the Phanerozoic, with an average volume greater than $2\times10^6 km^3$ and a peak activity at ~200 Ma, thus identified as the trigger of the mass extinction that brands the Tr-J boundary (Marzoli et al., 1999; Verati et al., 2007). It is associated with the breakup of the supercontinent, Pangea. CAMP volcanism is mainly represented by sills, lava flows and tholeiitic dykes characterized by low TiO2 concentrations, and relatively low SiO2. CAMP lava flows can be found across four continents: Northeastern South America and Eastern North America, Northwestern Africa and Southwestern Europe (Fig. 1a). Geochemical data from these different continents suggests that CAMP lavas are mostly similar in composition (Marzoli et al., 1999; Marzoli et al., 2004).

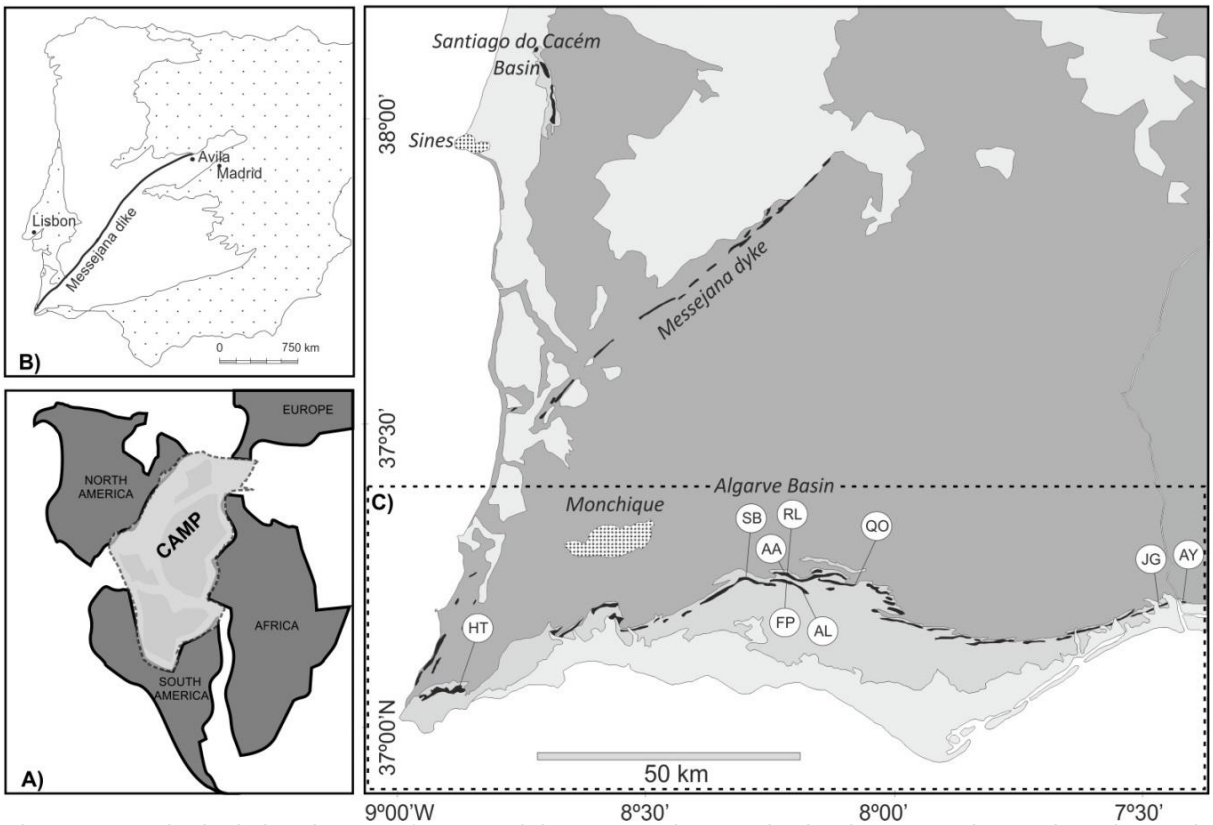

Figure 1: Geological sketch map of CAMP. (A) Preserved Central Atlantic Magmatic Province (CAMP) across four continents. The gray line delimits the probable extent of CAMP lavas at the time of its extrusion. (B) Simplified geological map of Iberia. (C) Map of southern Portugal. The dark lines indicate the main representations of CAMP, which includes the Messejana dyke and the Algarve and Santiago do Cacém's basins. The balloons at the Algarve's basin represent the sampling locations.

One of the best preserved and complete CAMP lava sequence (with outcrops thickness reaching 300 m) are found in Morocco, northwestern Africa and at the Newark basin, eastern North America. In Morocco, four primary units from CAMP volcanism were perfectly distinguished: The lower unit, intermediate unit, upper unit and recurrent unit (Knight et al., 2004; Marzoli et al., 2004) (Fig. 2).

In Newark basin, a thick and complete section was recovered and represents nowadays the best geomagnetic polarity time scale (GPTS) covering the late Triassic- earlier Jurassic period (Kent and Olsen 1999). The Tr-J boundary is assumed to be at ~202 Ma at the superchrone E24n, but the oldest CAMP lavas are identified ~40 kyr above this boundary, obviously refuting the role of CAMP on the

mass extinction (Kent and Olsen 1999) (Fig. 2). These authors also identified a very short reversal polarity (E23r) just below the Tr-J boundary, allegedly found on CAMP lavas in Morocco and correlated to the reversal E23r (Knight et al., 2004) (Fig. 2). This discovery would put an end on the recurrent discussion about whether or not CAMP was the trigger of the mass extinction. However, on my degree project and further published article, (Font et al., 2011) we were able to prove that the reversal found by Knight et al. (2004) was due to chemical remagnetization.

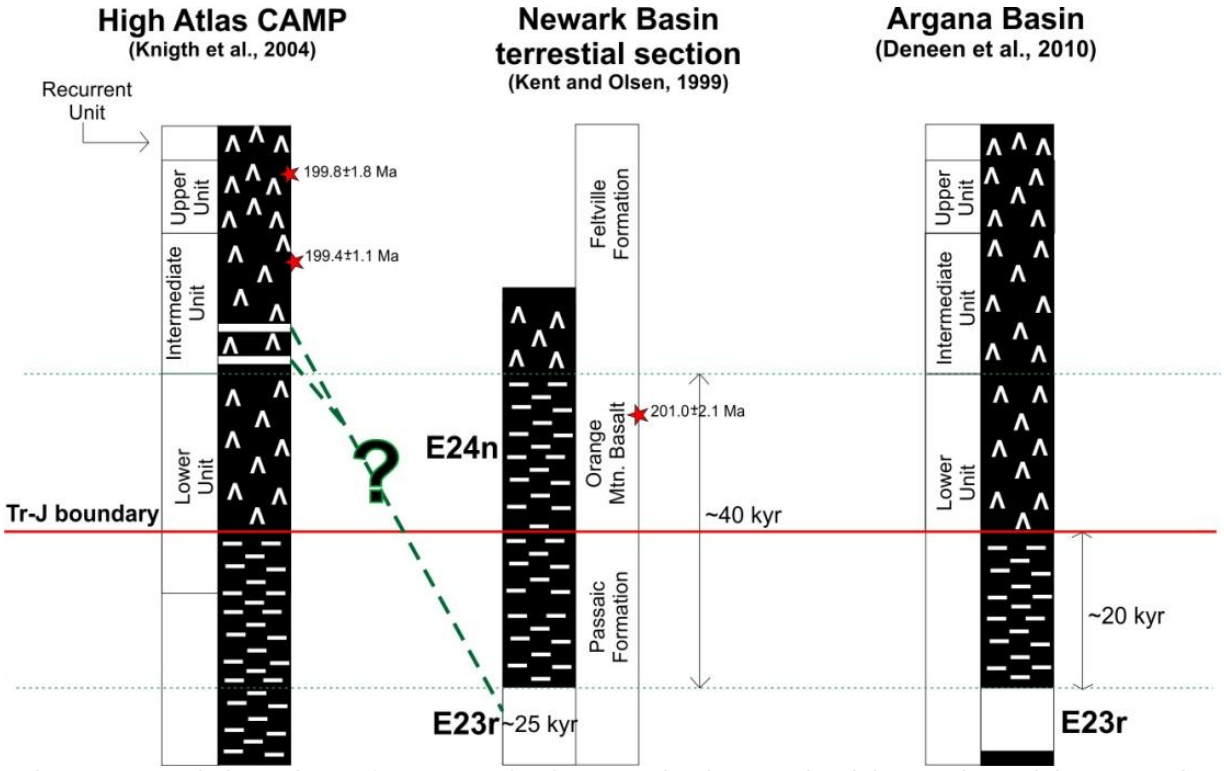

Figure 2: Correlation scheme for trans- Atlantic CAMP basins. On the right are showed the reversals found by *Knight et al., 2004* and its comparison with the Newark basin. On the left, is presented the magnetostratigraphy of Argana basin and its comparison with the Newark basin. The reverse "V" represents the CAMP lavas. The white boxes represent clay.

Recent studies conducted at the Argana basin reveals that the oldest CAMP lavas found at the Newark basin are correlated to the second pulse of CAMP volcanism (intermediate unit) found at Morocco, which means that the first volcanic pulse (lower unit) have not reached US and puts the oldest CAMP lavas of Morocco at ~20kyr above the Tr-J boundary instead (Deneen et al., 2010) (Fig. 2). The authors support the hypothesis of Phanerozoic mass extinction due to the emplacement of this LIP.

2.2 CAMP (Portuguese basins: studied area)

The preserved CAMP lava flows in Portugal are found at the Algarve basin, at the Santiago do Cacém basin (Fig. 1c) and in the Spanish Central System, where is located the Messejana dyke (Verati et al., 2007; Palencia- Ortas et al., 2006).

The Algarve and Santiago do Cacém basins comprises a basal sequence of continental sediments, namely siltstones and limestones of Hettangian age (Youbi et al., 2003) on which CAMP volcanic products were emplaced among thin layers of limestones and dolomites, suggesting synchronism between the volcanism and sedimentation (Martins et al., 2007). At the top of the sequence, the

volcanic products are covered by a thick Early Jurassic limestone layer. These volcanic products are mostly represented by subaerial lava flows, pyroclastic deposits and peperites (Martins et al., 2007) (Fig. 3).

In terms of geochemical composition, the Portuguese lava flows are classified as low Ti- tholeiitic basalts enriched in large ion lithophile elements, which suggests partial melting of heterogeneous mantle sources (Martins et al., 2007). Comparison with the Moroccan sequence suggests that Algarve basin outcrops are relatively homogeneous and similar to the Moroccan intermediate and upper unit (Marzoli et al., 2004; Rapaille et al., 2002) (Fig. 3). Recent 40Ar/39Ar data on the Portuguese volcanic units yields an age close to the Tr-J boundary with a mean value of 198.1 ±0.4 Ma. This age is correlated to the recurrent unit of the Moroccan basins and suggests a synchronous rifting and volcanism on both Southwestern Europe and Northeastern Africa (Marzoli et al., 2004; Verati et al., 2007).

The SW-NE oriented dyke of the Messejana (Fig. 1b) is also coeval with the age of the CAMP's outcrops (202.8±2.0 Ma).It comprises dolerite intrusions that obliquely cut the Hercynian basement for more than 530 km from South Portugal (Alentejo) to Central Spain (Avila). Palencia Ortas et al. (2006), conducted a paleomagnetic study on 40 sites within the dyke which yielded a reliable paleomagnetic pole for the Iberian microplate at: Plat=70.4º, Plong=237.6ºE (K=47.9, A95=3.5º). However, no paleomagnetic investigation has been conducted in the Portuguese CAMP lavas yet.

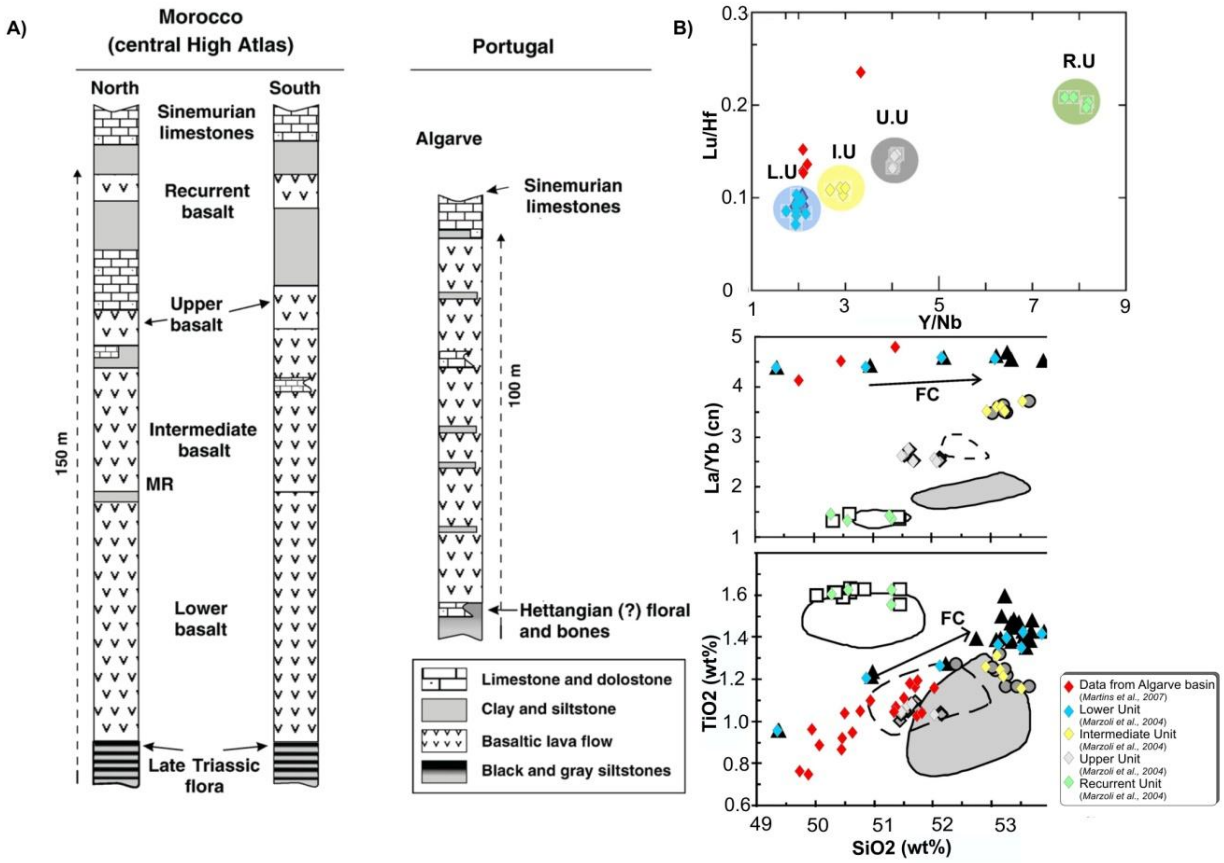

Figure 3: (A) Schematic stratigraphy of Moroccan and Portuguese outcrops and associated sedimentary layers (c.f. *Verati et al., 2007*). (B) Comparison of the major and trace elements compositions between Moroccan lavas and our samples (c.f. *Marzoli et al., 2004*).

3. Sampling

Samples were collected at nine sites within the E-W elongated Algarve basin using a portable gasoline-powered drill and oriented using a magnetic and solar compass. Eight to nine cylinders were collected at nine localities (e.g. "sites", Fig. 1c). The samples collected in the field were subsequently cut in the laboratory into standard specimens (2.2 cm in length × 2.5 cm in diameter) yielding 280 samples for future paleomagnetic measurements (Fig. 4).

Figure 4: Field pictures from the Algarve basin's outcrops. The magnetic and solar compass and the driller used to collect the samples (at the top). Inclinometer and the hammer used to mark the separation between two different lava layers, useful to estimate bedding corrections (at the bottom).

4. Methods

4.1 Petrography

Petrographic analyses were carried out in fresh specimens in order to discriminate the mineral content and textural features. Thin sections of a selected paleomagnetic sites (AA, AL, SB, FP; Fig.1c) were performed at the geology department's laboratory to later on be observed on an optical microscope under the supervision of Dr. Línia Martins.

4.2 Isothermal Remanent Magnetization (IRM)

Isothermal Remanent Magnetization (IRM) is one of the most used rock magnetic technique to identify the magnetic minerals present in a sample based on their coercivity. Common mineral such as magnetite or pyrrotite (ferromagnetic) have low coercivity values, whereas antiferromagnetic minerals such as hematite and goethite have much higher coercivity values. Furthermore, the amplitude of the magnetization saturation (SIRM) informs about the concentration of these magnetic minerals for a fixed volume.

Robertson & France (1994) and Kruiver et al (2001) showed that IRM acquisition curve theoretically follow a log normal distribution and are cumulative in intensity. The authors suggested that IRM curves can be approximated by a cumulative log-Gaussian (CLG) function, described by 3 parameters: $B_{1/2}$, SIRM and DP. DP is the dispersion parameter which reflects the distribution of the apparent

coercivities of a mineral phase and which can be interpreted in terms of homogeneity/heterogeneity of grain size and/or composition of a set of sample. Since IRM curve is the sum of each individual CLG's functions, this method allow the discrimination of each magnetic phase in the case of mixture. For example, basalts are frequently constituted by magnetite and hematite, which can be easily identify using the CLG function.

Representative samples were previously demagnetized by an alternated magnetic field (AF) at 100 mT and further submitted to a progressive uniaxial and constant magnetic field up to 1 T at constant temperature, using a pulse magnetizer (ASC Scientific IM-10-30). For the CLG treatment we used the Kruiver et al (2001) software which allows fitting (by tentative and error) of $B_{1/2}$, SIRM and DP values on a linear (LAP), gradient (GAP) and probability (SAP) scale. If more than one mineral phase is present, it is expected the theoretical curves to be fitted by more than one component.

4.3 Thermomagnetic Analysis

Thermomagnetic curves were performed in order to identify the ferromagnetic minerals based on their Curie temperature. Curie (Néel) temperature is unique for a particular mineral and therefore is commonly used to identify its composition. For example, magnetite has Curie temperature of 580ºC and can also be identified at low temperature measurements by its Verwey transition in the case of very fine grained magnetite (a hump in magnetic susceptibility at ~-120ºC due to atoms rearrangements). Magnetite with higher content of titanium (Ti-rich titanomagnetite) has lower Curie temperatures on the order of ~200ºC whereas for a Ti-poor titanomagnetite Curie temperatures are ~560ºC. Hematite, on the other hand, has Néel temperatures (the equivalent of Curie temperature for antiferromagnetic minerals) much higher than magnetite (~680ºC) and its titanium content also influences its Néel temperature.

Magnetic susceptibility is measured at high and low temperature. The low temperature (LT) measurements are performed on a CS-L cryostat apparatus which uses liquid nitrogen to cool down the equipment. Magnetic susceptibility is measured while the apparatus is warming up from -192ºC (e.g., temperature of the liquid nitrogen) up to the room temperature. The high temperature (HT) measurements are performed on a CS4 furnace in an Argon controlled atmosphere from the room temperature until 700ºC. Subsequently, magnetic susceptibility is measured while the equipment is cooling down from 700ºC to room temperature. Both measurements were performed using a MFK1 Kappabridge at the Laboratory of Paleomagnetism of the IDL. Data were treated by the Cureval 8.0 (AGICO) software. Later on, an approach to calculate the Curie temperature of ferromagnetic minerals presented on the rock is performed using the inverse susceptibility method proposed by Petrovský and Kapricka (2006).

4.4 Hysteresis data

The ferromagnetic minerals have a unique capacity to record the direction of an applied magnetic field. Unlike paramagnetic or diamagnetic minerals, when the applied field is removed, the ferromagnetic minerals will not return to zero and the offset from the origin is called magnetization of remanence, M_{rs} which is a record of the applied magnetic field. The path of the magnetization, J with respect to the applied field, H is perfectly explained by the so called Hysteresis loop.

Hysteresis parameters have been extensively used to unravel the grain size of the magnetic carriers. The Day plot was first proposed by Day et al. (1977) and is widely used in paleomagnetism to discriminate the domain state (single domain, SD; pseudo-single domain, PSD; multidomain, MD) of the magnetic carriers. It is based on the ratio of hysteresis parameters ($M_{rs}/M_s \times H_{cr}/H_c$) where M_{rs} is the maximum saturation remanence; Ms is the maximum saturation magnetization; H_{cr} is the remanent coercive force (e.g. the field needed to reduce M_{rs} to zero) and H_c is the bulk coercivity. The theoretical bounds of the Day plot are defined by: $M_{rs}/M_s>0.5$ and $H_{cr}/H_c<5$ for the SD region; $0.5> M_{rs}/M_s>0.05$ and $1.5< H_{cr}/H_c<5$ for the PSD region and $M_{rs}/M_s<0.02$ and $H_{cr}/H_c>5$ for the MD region.

The importance of this method relies on the necessity to know whether or not the paleomagnetic samples contain SD magnetite since the latter are the best recorder of the ancient Earth's magnetic field. This is because SD and even PSD (pseudo-single-domain) particles have higher coercive force, H_c than MD grains (Butler 1996).

More recently, Dunlop et al., 2002 developed a theoretical day plot curve for magnetite for each domain state and admixtures of magnetic grains (MD+SD; SD+SP). The main problems related to these theoretical curves rely on the fact that the hysteresis parameters are not exclusively a function of the domain state. Mineral composition, mixture of different minerals or minerals with different domain state, thermal activation and magnetostatic interaction may lead to erroneous interpretations of Day diagrams.

Roberts et al. (2000) developed a new method to discriminate the domain states, claiming that the use of Day plot diagrams can often leads to misinterpretations of the data. In this article, Roberts et al. (2000) present a new tool (FORC diagrams) not only to identify the magnetic domains (SD, SP, PSD and MD grains) but also to reveal whether or not magnetic interaction is present. FORC's diagrams are obtained after submitting a sample to a saturating magnetic field (H_b) and then, decrease the field to a reversal magnetic field (H_a). First Order Reversal Curves (FORC) is defined as the resultant magnetization curve between H_a and H_b. This measurement was repeated for different reversal fields yielding a set of FORC (for each reversal field) that fills the inside of a hysteresis loop. The FORC diagram, mostly used, is a contour plot of a FORC distribution displayed on a Hu [Hu=(Ha+Hb)/2] versus Hc [Hc=(Hb-Ha)/2] plot, where Hc represents the coercive force of the magnetic grains on the specimen and Hu is the local interaction field.

For the present study, hysteresis measurements and FORC diagram were performed at nine characteristic samples from each paleomagnetic site. The measurements were performed using a Vibrating Sample Magnetometer (VSM) with a maximum applied field of 1T at the University of Marie Curie, Paris. Dunlop's theoretical curves are used for comparison of hysteresis parameter.

4.5 AF cleaning

The specimens were subjected to a progressive alternating magnetic field (AF demagnetization) using a LDA-3A demagnetizer from 0 (Natural Remanent Magnetization, NRM) up to 100 mT. This process is used to eliminate low-field secondary magnetizations that the rock might have acquired subsequent to its formation and to identify the direction of the original remanent magnetization recorded in the rock during its formation. At each AF demagnetization step, the remanence is measured using a JR6 magnetometer. Principal Component Analysis (Kirschvink, 1980) and Fisher statistic (Fisher, 1953) are then used to calculate the direction of the Characteristic Remanent Magnetization (ChRM). These calculations are made by using the REMASOFT software (AGICO).

A total of 280 specimens were submitted to AF cleaning for which 257 specimens gave reliable directions that were used to calculate the characteristic remanent magnetization (ChRM). Erroneous data "Outliers" were eliminated using the Vandamme (1994) cutoff angle method which is based on a recursive method that optimizes the probability of finding the true mean direction.

The paleomagnetic pole is calculated either using mean ChRM direction computed for all samples or for all sites. Reliability of the final paleomagnetic pole is evaluated using the Q criteria of Van der Voo (1990). Comparison of the paleomagnetic pole with other referenced pole is made by using the McFadden and Lowes (1981) test.

5. Results

This section will be subdivided into two main groups: magnetic mineralogy and paleomagnetic results. The first approach is to show if the primary magnetic mineralogy has been preserved since rock formation or if it has been altered by chemical processes. Paleomagnetic results will provide new geochronological data (through the magnetic polarity recorded by the rocks; e.g. magnetostratigraphy) and a new paleomagnetic pole and its eventual use for paleogeographic reconstructions will be discussed by comparison with the key pole of the Messejana dyke and CAMP lavas from Morocco.

5.1 Magnetic mineralogy

Rock magnetic studies are essential to identify the dominant magnetic carriers presented in paleomagnetic specimens. It is of extreme importance to infer whether or not there is preservation of the primary magnetization otherwise, the paleomagnetic studies would be useless to reconstruct the global paleogeography of the Earth plates.

In this subsection, powerful tools are used to constrain the nature, grain-size, origin and type of ferromagnetic minerals characteristic of the CAMP basalts from Portugal, namely: petrography, IRM (Isothermal Remanent Magnetization), Thermomagnetic analysis and Day plot and FORC's (First Order Reversal Curves).

5.1.1 Petrography

Algarve lava flows are porphyritic rocks with a characteristic aphanitic texture, mainly due to its fast cooling which prevent the growth of the minerals. The samples are characterized by the presence of few phenocrystals developed in a matrix of finer grains. The samples showed a simple mineralogy mainly dominated by plagioclase, clinoperoxenes, feldspaths and opaque minerals (Fig. 5).

The opaque crystals correspond to ferromagnetic minerals. Their preserved subeuedric morphology suggests primary origin.

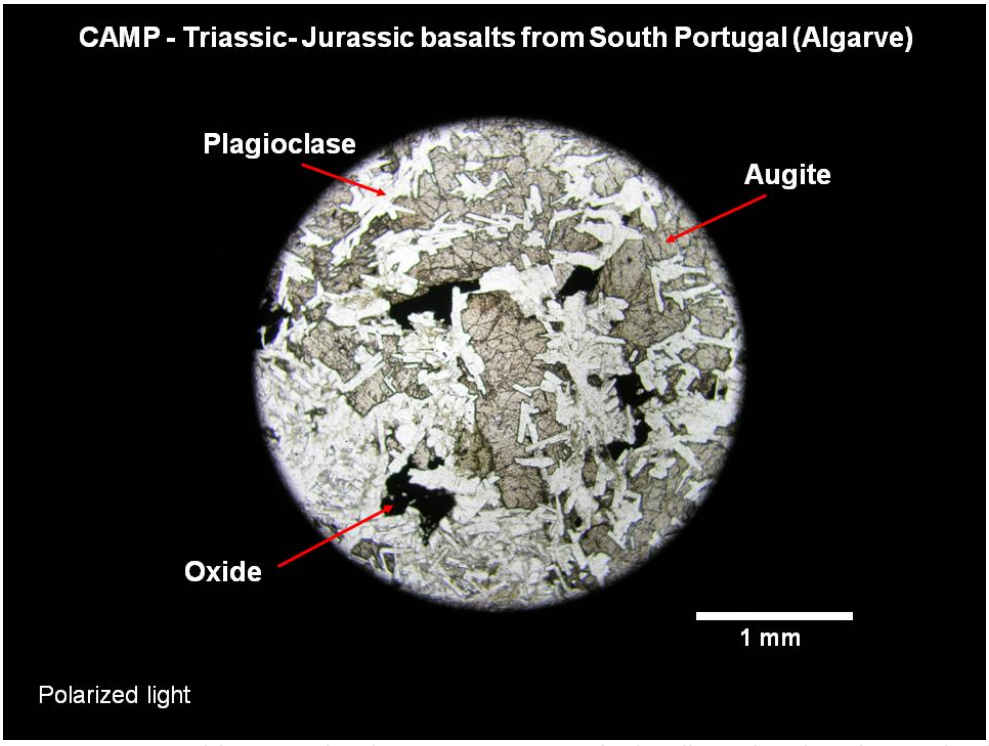

Figure 5: Petrographic example of CAMP's outcrops (AL) collected at the Algarve' basin.

5.1.2 IRM acquisition curves

A total of 34 samples (2 to 12 per paleomagnetic site) were analyzed. All studied samples display a similar behavior during the gradual acquisition of uniaxial isothermal remanent magnetization (IRM). Saturation (SIRM) in most samples is reached below 100mT suggesting a low coercive phase as the dominant magnetic carrier (magnetite?) despite the presence of a higher coercive phase (hematite?) at few samples which do not attain saturation (Fig. 6).

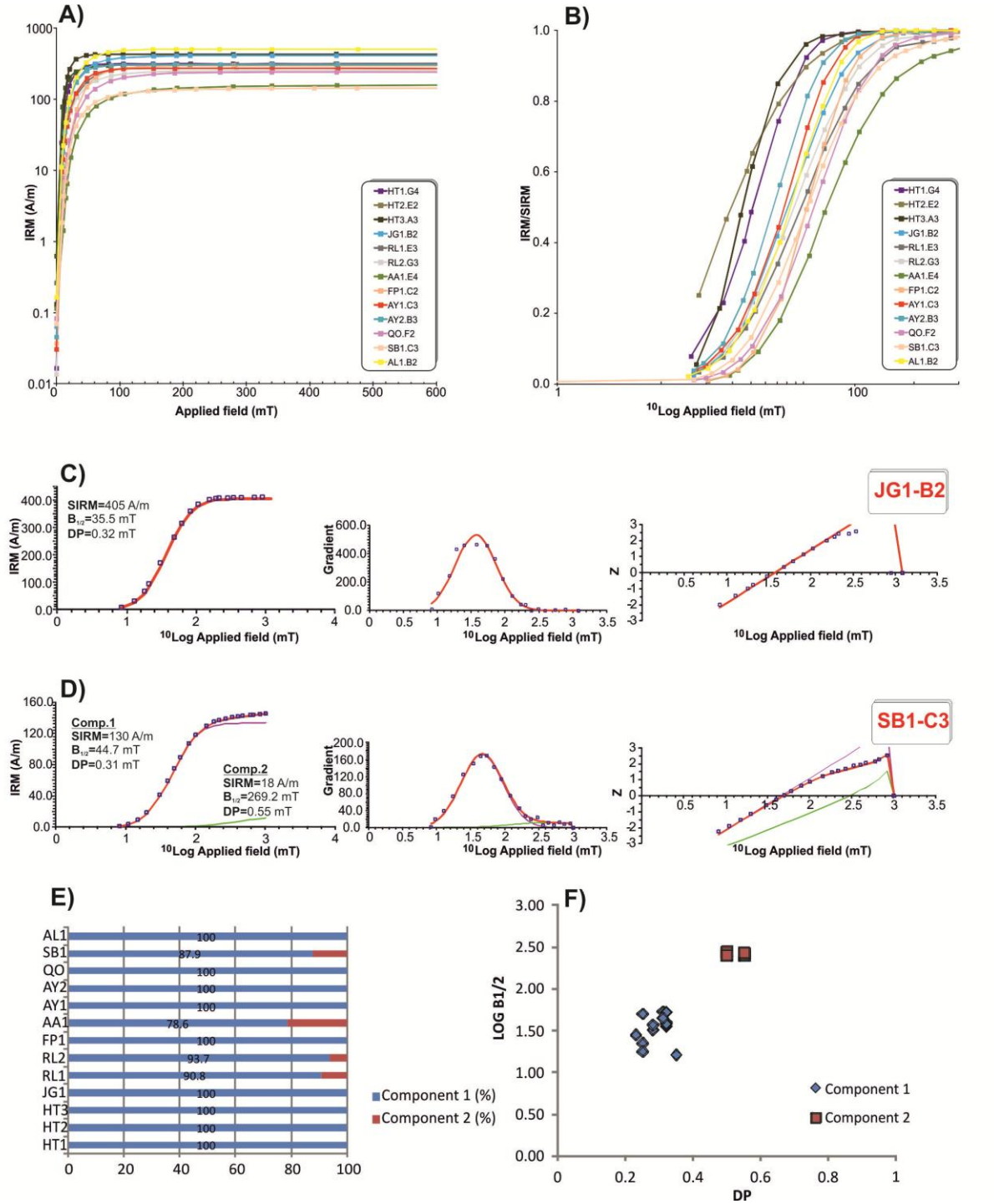

Figure 6: Isothermal remanent magnetization (IRM) analysis. (A) IRM vs. Applied field. (B) IRM/SIRM vs. Log Applied field. (C) and (D) Examples of analysis treated by the cumulative log-Gaussian function (*Kruiver et al., 2001*). (E) Contribution of different magnetic phases on the samples. (F) Comparison of the ratio DP vs. log $B_{1/2}$.

SIRM values vary between 130 A/m (SB1.C3) to 500 A/m (AL1.B2) and reflect significant differences in concentrations of ferromagnetic minerals (Fig. 6A; Table 1). Once representing IRM data on a logarithmic scale for the induced field (H in mT; Fig. 6B) significant differences in B1/2 values (field needed to reach half of the saturation) are observed ranging from 16.2 mT (HT2.E2) to 53.7 mT (AA1.E4; Table 1).

After treatment by the cumulative log-Gaussian function (CLG) using the Kruiver's software (Kruiver et al., 2001), it is shown that almost all samples display a unimodal distribution, despite the presence of bimodal distribution at some samples (Fig. 6C; Fig. 6D). The unimodal distribution (e.g. JG1.B2; Fig 6C) is characterized by a single Gaussian curve for which SIRM values lie between 240 A/m (QO.F2) and 500 A /m (AL1.B2; Table 1) and the mean coercivity fields with ranges of 16.2 mT (HT2.E2) to 52.5 mT (QO.F2). Through the values of SIRM and bulk coercivity of this distribution, it is possible to infer that the mineral presented in those samples is of low coercive phase, possibly magnetite (Dunlop and Özdemir, 1997; Lowrie, 1997).

Table 1: SIRM, $B_{1/2}$ and DP estimates for characteristic samples using the *Kruiver* software

	Componente 1				Componente 2			
Samples	**SIRM**	**B1/2**	**DP**	**%**	**SIRM**	**B1/2**	**DP**	**%**
HT1.G4	312	22.4	0.25	100				
HT2.E2	305	16.2	0.35	100				
HT3.A3	430	17.8	0.25	100				
JG1.B2	405	35.5	0.32	100				
RL1.E3	295	39.8	0.32	90.8	30	251.2	0.55	9.2
RL2.G3	239	38.0	0.32	93.7	16	275.4	0.50	6.3
FP1.C2	297	50.1	0.25	100				
AA1.E4	132	53.7	0.31	78.6	36	251.2	0.50	21.4
AY1.C3	269	32.4	0.28	100				
AY2.B3	300	28.2	0.23	100				
QO.F2	240	52.5	0.32	100				
SB1.C3	130	44.7	0.31	87.9	18	269.2	0.55	12.2
AL1.B2	500	37.2	0.28	100				

Bimodal distributions are also found at some samples. (e.g. SB1.C3; Fig. 6D) Non-saturated curve is easily observable on GAP and SAP diagrams. As IRM acquisition curve are linearly added, if more than one magnetic phase is present, mixtures are immediately denoted by the presence of more than one Gaussian curve (GAP diagram) and deflections of the distribution (SAP diagram). Two magnetic phases are present: a low coercivity phase, with SIRM values on the hundreds order and coercivity values similar to those found at the unimodal distribution. This low coercive phase, presented in all samples, is thought to be magnetite and contributes with more than 80 % to the total remanence while the higher magnetic phase reaches ~20% maximum of the IRM signal (Fig. 6E). The higher coercive phase is characterized by much lower SIRM values ranging from 16 A/m (RL2.G3) to 36 A/m (AA1.E4; Table 1) and coercivities significantly higher than the low coercive phase, ranging between 251.2 mT (RL1.E3; AA1.E4) to 275.4 mT (RL2.G3). The strong similarity of $B_{1/2}$ and DP values for both component 1 and component 2 in all specimens suggests the presence of homogeneous populations of the soft (lower coercivity) and hard (high coercivity) magnetic fractions in terms of composition and grain size (Fig. 6E). The CLG parameters of the Portuguese CAMP lavas are strongly similar to those found in the CAMP lavas from Morocco (Font et al., 2011) confirming primary (magmatic) origin for these minerals.

5.1.3 Thermomagnetic Analysis

Considering that several minerals such as magnetite and pyrrhotite, goethite and hematite have similar maximum coercivities, (Lowrie, 1997) interpretation of IRM acquisition curves alone, cannot be used to identify the composition of the magnetic carriers. In order to do that thermomagnetic analyses of representative samples (1 per paleomagnetic site). Just like IRM measurements, among all the measured thermomagnetic curves, merely two different behaviors are found and illustrated (Fig. 7).

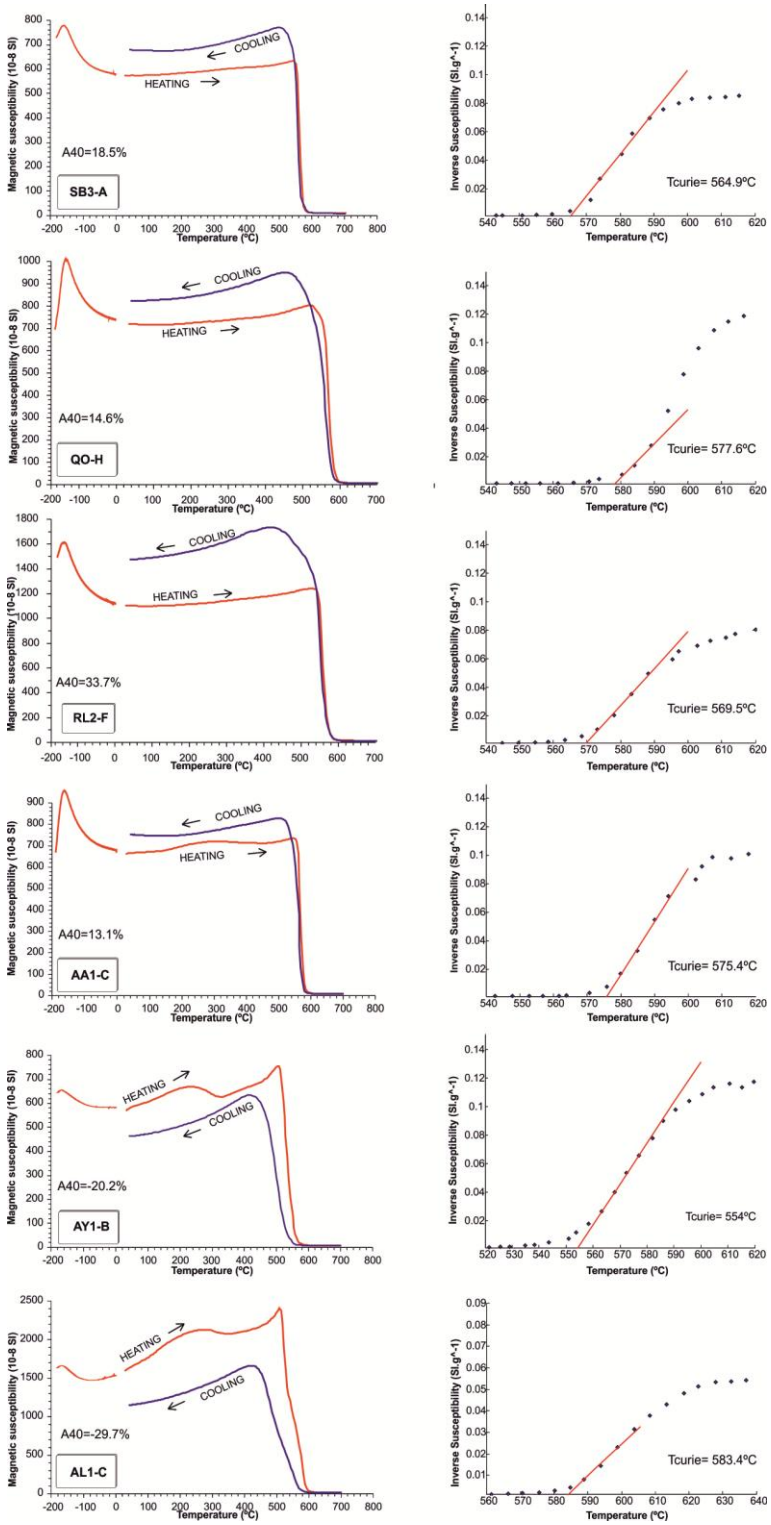

Figure 7: Low and High temperature thermomagnetic curves (on the left) and the respective inverse susceptibility method (on the right).

Curie temperatures are calculated using the inversion method of Petrovský and Kapricka (2006). According to Curie temperatures, two distinct groups of samples can be recognized. Group A, (e.g. SB3-A; QO-H; RL2-F; Fig. 7) characterized by a single ferromagnetic phase with Curie Temperatures ranging from 564.9º to 577.6ºC (Fig. 7), compatible with Ti-poor titanomagnetite (Dunlop and Özdemir 1997). The positive alteration index characteristic of this group suggests formation of new mineral during the heating process, most likely magnetite (Hrouda et al., 2002; Hrouda 2003). Group B, (e.g. AY1-B; AL1-C; AA1-C; Fig. 7) characterized by the presence of at least two magnetic phases where Ti-poor titanomagnetite is the dominant with Curie temperatures ranging from 554ºC to 583ºC. A hump at ~240ºC to 320ºC is observed during the heating process (AA1-C; AY1-B; AL1-C; Fig.7) but is no longer observed on the cooling curve (Fig. 7). This behavior is interpreted as the result of titanomaghemite instability during heating (Dunlop and Özdemir 1997) resulting on the inversion to a multiphase mixture of magnetite, ilmenite, pseudobrokite and other minerals (Dunlop and Özdemir 1997, Özdemir, 1987). The positive alteration index in some samples, suggest the inversion of titanomaghemite into newly formed magnetite (AA1-C; Fig. 7) while others (AY1-B; AL1-C; Fig. 7) are characterized by negative alteration index which suggests the disintegration of the original mineral phase into lower susceptibility residual phase (Hrouda et al., 2002).

Verwey transition is present in all samples (Fig. 7) and branded by the typical hump at ~ -150ºC, characteristic of structural changes on magnetite (Dunlop and Özdemir 1997, Özdemir et al, 1993). The magnitude of the Verwey transition for the samples on the group A is markedly higher than for the samples on the group B. As the samples from the group B suffered from low-oxidation processes, (i.e. maghemetization) the Verwey transition is suppressed which leads to this clear difference on the magnitude of the transition in both groups (Özdemir et al., 1993).

5.1.1 Hysteresis data

Coercivity and remanence ratios (M_{rs}/M_r and H_{cr}/H_c) were plotted on the theoretical curve of Dunlop et al. (2002) (Fig. 8). All data fall on the left region of the SD and MD mixture of the modified day plot (Dunlop, 2002) with values ranging between 1.86 and 3.42 for the coercivity ratios and between 0.07 and 0.25 for the remanence ratios (Fig. 8).

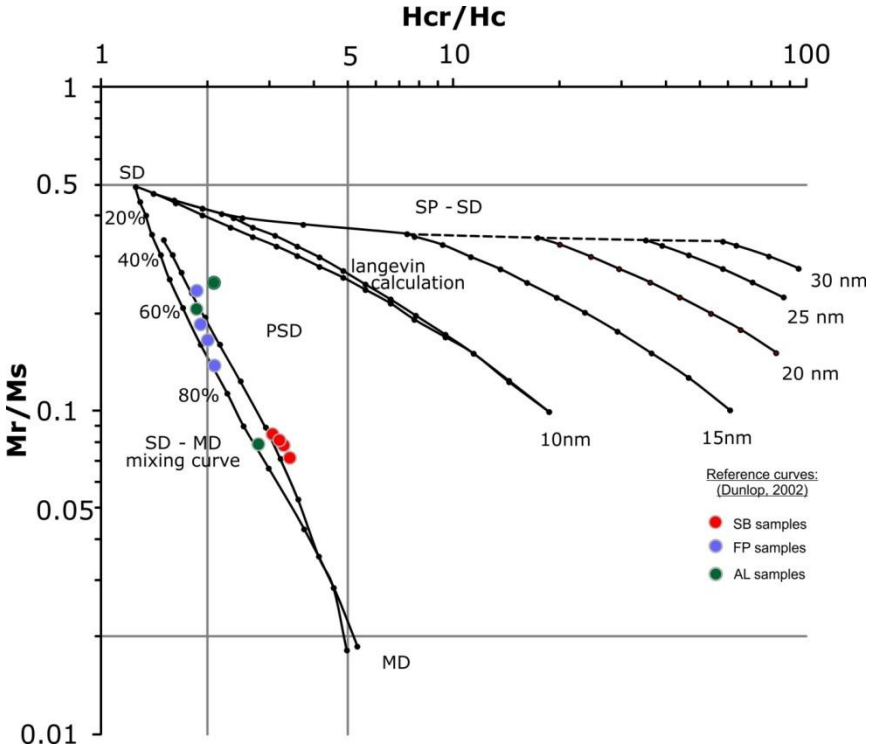

Figure 8: Modified Day plot showing the domain state of CAMP samples compared with theoretical mixing curves (*Dunlop, 2002*)

It is interesting to note that all SB samples have the lowest remanence ratios and the highest coercivity ratios while all FP samples closely follows the SD+MD mixing curves toward higher remanence ratios. According to the literature, this could mean that FP samples have magnetites with lower grain size than SB samples. On the other hand, AL samples apparently have a larger range of grain sizes. This SD+MD mixture is typical of basalts which cools fast enough so that the grain size of the opaque minerals is typically of few µm but also may carry larger grains due to growth when the lava flows are thick enough.

5.1.1 FORC's

Three characteristic FORC diagrams are shown which are representative of the typical behaviors found on the 6 analyzed samples (Fig. 9).

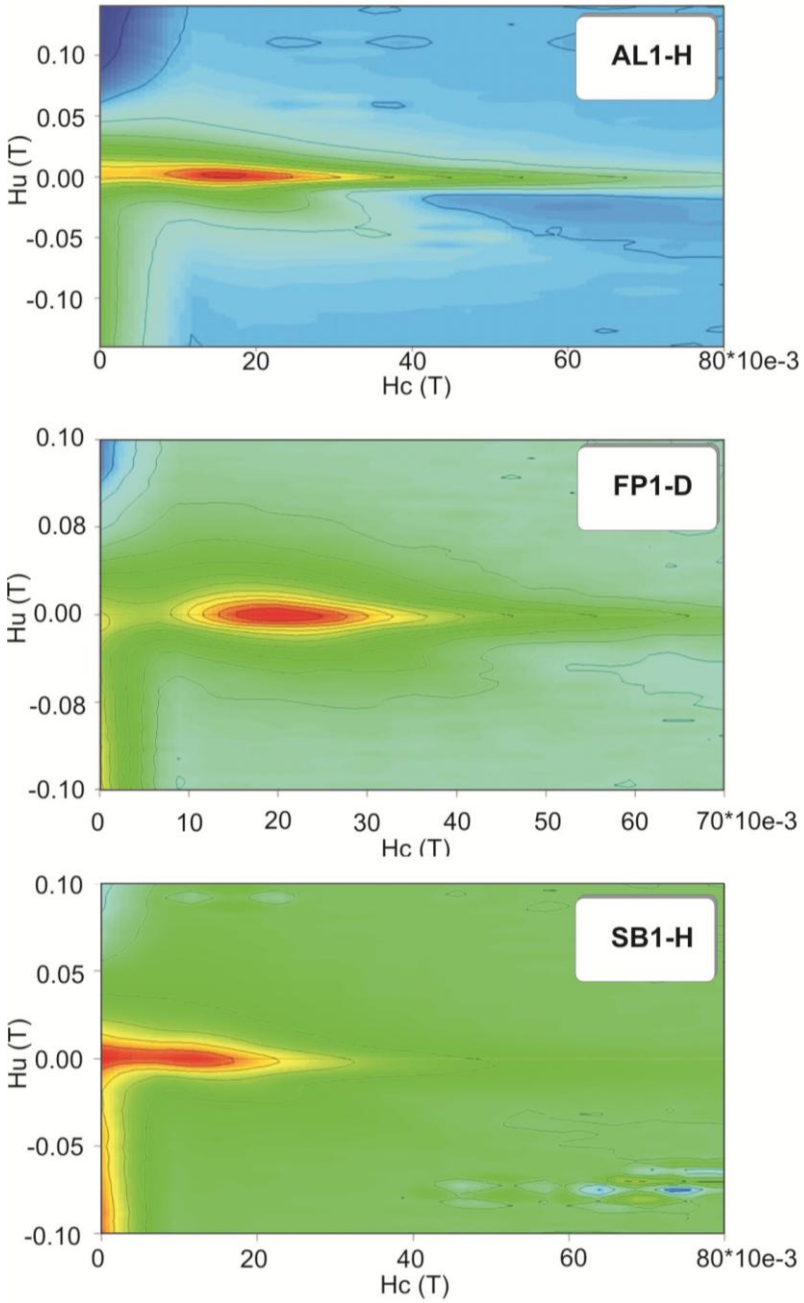

Figure 9: FORC diagrams for characteristic samples.

AL1-H sample (Fig. 9) displays a narrow distribution, slightly above the origin of the magnetic interacting field (Hu), suggesting the existence of interaction between the magnetic particles. The mean coercivity field (Hc) value has a peak distribution at ~17 mT, which is slightly below of what is expected for a pure SD magnetite (Dunlop and Özdemir, 1997, Muxworthy et al., 2002). The displacement of Hc to lower values and the presence of vertical contours in the lower-left part of FORC's distribution, (practically parallel to Hu axis) suggest magnetic interactions between SP and SD particles. Conversely, FP1-D (Fig. 9) displays a typical non-interacting SD particle with close contours at Hu=0 and a peak distribution of coercivity field at ~20mT. However, the presence of a second peak at the origin (Hi=0 and Hc=0) with a shape similar to AL1-H leads to the conclusion that SP particles are also present in this sample.

SB1-H sample (Fig. 9) is very similar with AL1-H sample (Fig. 9). The largest displacement toward lower coercivity field values (~7 mT) and a slight shift above Hu=0 suggests that SP and SD particles are present on the sample, both with similar intensities.

All FORC's distributions suggest a SD+SP mixture for the analyzed samples. Conversely, day plots strongly follow the SD+MD trend, but on these samples, there are no evidences of MD-like behavior.

In order to verify if SP particles are present, such has been suggested by FORC analysis, we have conducted Kfd analysis. The Kfd is a proxy to evaluate the contribution of superparamagnetic particles within the bulk mineralogy (Dearing et al., 1999). For low frequency measurements (klf), the SP grains close to the boundary of SD grains, contributes to the bulk susceptibility whilst at high frequency measurements (khf) does not. Our results show no SP contribution, consistent with Day plot results (Table A1).

5.2 Paleomagnetic Results

A total of 280 samples were demagnetized at the IDL laboratory using AF treatment. Most samples yielded stable demagnetization patterns at high fields. More than 90% of the remanence is demagnetized between 40 mT (JG samples) and 100 mT, (SB samples) suggesting a low to medium coercive phase as the dominant magnetic carrier (Fig. 10).

Zijderveld diagrams (orthogonal diagrams) show the presence of two magnetic components: a high field remanence projected to the origin of the diagrams, and a lower coercivity component, interpreted as a secondary viscous (VRM) magnetization which is successfully removed with fields lower than 20 mT (Fig. 10).

Natural Remanent Magnetization (NRM) intensity lies between 0.4 A/m to 13.5 A/m, typical of basalts (Dunlop and Özdemir, 1997), despite the wide range of intensity which may be due to superficial chemical alteration and to error associated to the volume of samples (some samples being fractured).

From the 280 samples, 257 were used to calculate the characteristic magnetic component (ChRM). Outliers were excluded based on the Vandamme (1994) cut-off by using the rotepole software (Ultreicht). All magnetic directions are positive (normal) with mean inclinations of 40º to 45º (Fig. 11). Mean ChRM (characteristic remanent magnetization) were calculated based on samples (sample-based mean direction) and on average direction per paleomagnetic site (site-based mean direction) (Table 3). Tilt corrections were applied to the data in order to correct for eventual post-tectonic movements. Tilt corrected sample-based mean direction yields: Dec=353.4º and Inc=52.8º (N=257, a95=1.5º, k=35.8) (Fig. 11B, left). Tilt corrected site-based mean direction yields: Dec=0º and Inc=50.4º (N=8, a95=8.3º, k=45.6) (Fig. 11B, right). After tilt correction (Fig. 11B) the dispersion parameter k is significantly higher (i.e. lower dispersion; k=45.6) than the non-corrected data (k=23.2; Fig. 11A) suggesting a pre-tectonic origin for the magnetization.

The paleomagnetic pole for the Portuguese CAMP basalts is calculated based on sample-and site-based mean directions, yielding: Plat=83.3º, Plong=236.1º (A95=1.8º; K=25.9) and Plat=84.4º, Plong=177.9º (A95=9.8º; K=32.9), respectively. For the calculation of the site-based pole, a Virtual

Geomagnetic Pole (VGP) is calculated for each paleomagnetic site, yielding a total of nine VGP's. Since the VGP's of the Ayamonte outcrops give unreliable directions (probably due to complex tectonics and deformation), only eight of these nine VGP's were selected (Table 3; Fig. 11C, right).

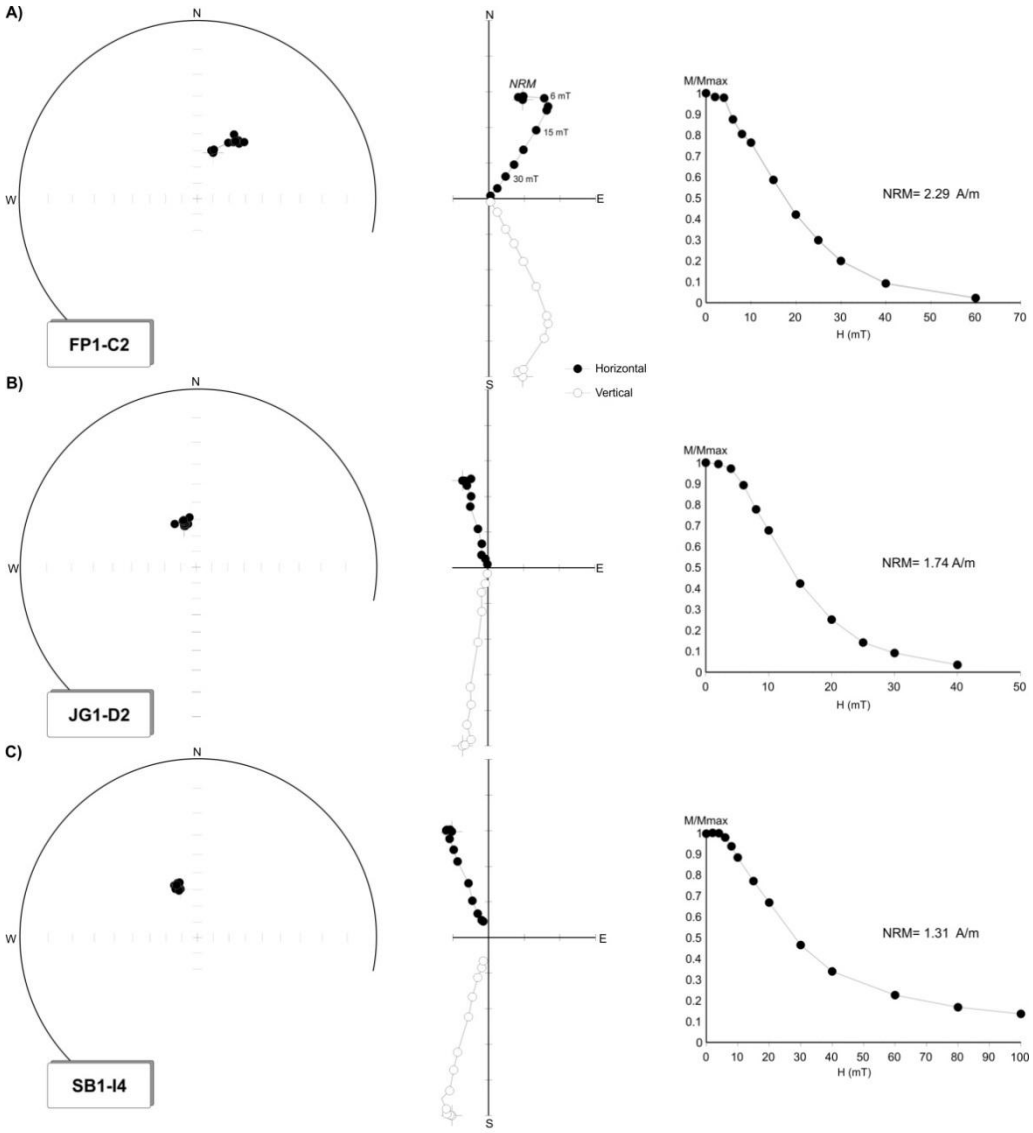

Figure 10: Paleomagnetic results for samples (A) FP1-C2, (B) JG1-D2 and (C) SB1-I4. Stereographic projection (on the left) and orthogonal projections and remanence intensity versus the demagnetizing field (on the right)

The fact that the site-based mean pole present high values of A95 is probably due to the existence of two distinct groups of direction (A and B components; c.f. Fig. 11), which are discussed later.

In order to check for the quality of a paleomagnetic pole, Van Der Voo (1990) proposed a useful set of seven reliability criteria, constituting the so-called Q-criteria (Table 2). Our new paleomagnetic pole passes 4 of the 7 criteria of Van Der Voo (1990), namely:

1. An accurate radiometric age for CAMP lavas provided by Verati et al. (2007);
2. Sufficient number of samples and adequate statistic parameters;
3. Adequate demagnetization (Fig. 10);
4. There is no overlap with poles from younger ages (Fig. 13);

Three criteria's are not fulfilled because: i) field tests are not conductible due to bad field exposure, ii) The structural and tectonic relations between Algarve basin and the Iberian plate are complexes and

poorly constrained by geological evidences and iii) CAMP volcanism occurred at ~200 Ma which is coincident with a large interval of normal magnetic polarities (Kent and Olsen, 1999; Fig. 2) and therefore, the presence of reversals is unlikely. However, we propose to substitute the reversal Q-criteria by our detailed magnetic mineralogy study, giving Q=5. A paleomagnetic pole with Q>3 is considered reliable.

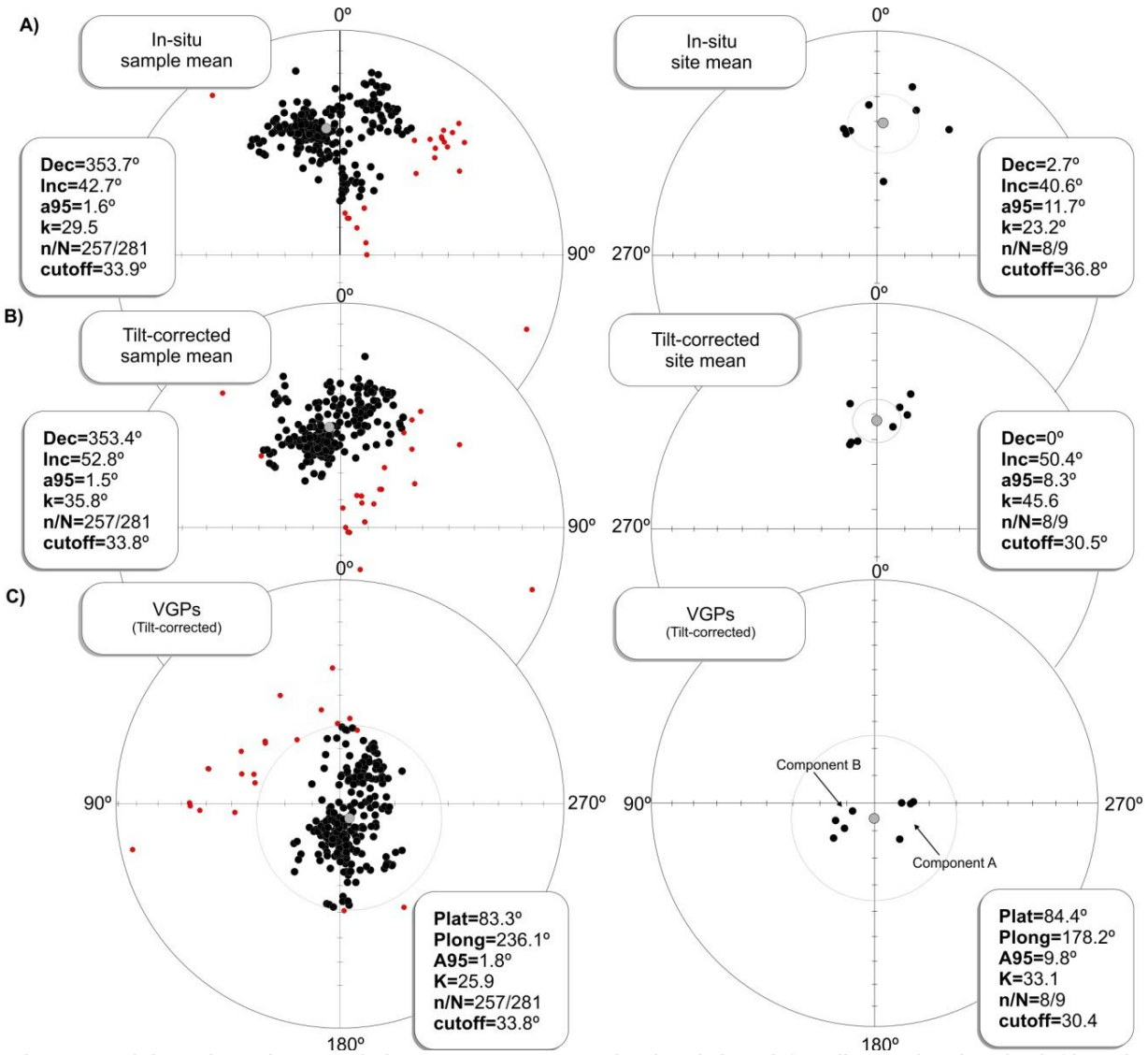

Figure 11: (A) In situ- Characteristic Remanent Magnetization (ChRM) for all samples (on the left) and per paleomagnetic site (on the right); (B) Tilt corrected ChRM. Sample (on the left) and site-based mean direction (on the right); (C) Corresponding Virtual Geomagnetic Pole (VGP) calculated using sample-means (on the left) and site-means (on the right).

Table 2: Reliability criteria for paleomagnetic data by Van Der Voo (1990)

Number	Brief description
1	Well-determined rock age and a presumption that the magnetization is the same age
2	Sufficient number of samples (N ≥24), k (or K)≥10, and a95 (or A95)≦16º
3	Adequate demagnetization that demostrably includes vector substraction information
4	Field tests that constrain the age of magnetization
5	Structural control and tectonic coherence with craton or block involved
6	Documented evidence of the presence of reversals
7	No resemblance to paleomagnetic poles of younger age

Table 3: Tilt corrected ChRM site-mean directions and corresponding VGP's. Lat/Long= site latitude/longitude; N= total number of samples n= number of samples used for mean calculation; Dec/Inc= declination/inclination; k/R/a95= fisher statistic parameters corresponding to dispersion parameter/resultant vector length/ 95% confidence circle, respectively. Plat/Plong= VGP Latitude/Longitude; Paleolat= Paleolatitude of the plate.

		Geographic coordinates(º)				ChRM(º)						VGPs (º)			
Area	Site	Lat.(N)	Long.(W)	Tilt correction	N	n	Dec	Inc	R	k	a95	Plat.	Plong.	A95	Paleolat
São Bartolomeu	SB	37.257	8.299	N80º/16º	117	107	343.3	57.1	106.51	214.9	0.9	76.8	296.5	1.2	37.7
Alte I (top)	AL	37.286	8.167	N290º/19º	23	20	10.6	44.4	19.9	188.1	2.4	75.8	129.7	2.3	26.1
Alte II (middle)	RL	37.235	8.176	N108º/28º	14	13	8.9	52.2	12.95	222	2.8	81.5	109.7	3.4	32.8
Caminho velho de Alte	FP	37.241	8.188	N170º/20º	22	22	14.9	46.6	21.56	47	4.6	74.4	113.5	5.6	27.9
Atalaia	AA	37.248	8.179	N120º/5º	25	25	13.8	38.4	24.91	261.8	1.8	70.4	130.3	1.8	21.6
Jardim del Gonduana	JG	37.226	7.410	N70º/14º	17	17	347.5	57.3	16.87	118.2	3.3	80.1	273.8	3.7	38
Hortas do Tabual	HT	37.073	8.876	N250º/0º	30	30	347.8	42.7	29.39	47.2	3.9	74.4	215.3	3.9	24.8
Quinta da Ombria	QO	37.194	8.018	N110º/28º	11	11	342	57.7	10.9	100.4	4.6	75.9	274.3	5.1	38.4
Ayamonte (Spain)	AY	37.228	7.404	N90º/15º	21	20	23.9	75.1	19.13	21.8	7.2	59.5	11.8	9.7	62

VGPs	N	Plat	Plong	K	A95
Sample-based mean	257	83.3	236.1	25.9	1.8
Site- based mean	8	84.4	177.9	32.9	9.8

6. Discussion

The results presented here give us new clues to i) investigate if the magnetic mineralogy of the Portuguese CAMP lava is preserved and suitable to provide a new paleomagnetic pole for Iberia at 200 Ma, ii) to test if this newly found pole is reliable for paleogeographic reconstructions, and iii) to provide magnetostratigraphic data for global-scale correlations with other CAMP section worldwide.

6.1 Magnetic mineralogy of the Portuguese CAMP lavas

Rock magnetic studies are essentials to understand the type and domain of the ferromagnetic mineral within the rock, but mostly, they are crucial to check if the samples are suitable for paleomagnetic studies. Despite the severe alteration of the entire Algarve's basin region already reported by previous geochemical studies (Martins et al., 2007; Verati et al., 2007) primary NRM directions seems to have been preserved.

Rock magnetic experiments conducted on the Portuguese CAMP lavas indicate the presence of a low to medium coercivity mineral, despite the accessory contribution of a higher coercivity in some samples (Fig. 6). The low to medium coercive phase corresponds to fine Ti-poor titanomagnetite as shown by typical Curie temperatures of 560º-580ºC (Fig.7). Thermomagnetic analysis clearly shows a Verwey transition at around -150ºC characteristic of magnetite. Presence of maghemite is also identified based on its inversion temperature observed at ~250-350ºC in some samples (Fig. 7). However, hematite is not depicted in our thermomagnetic curves indicating that it may be present only in very low content (Fig. 7).

Hysteresis parameters plotted on the modified Day plot (Dunlop, 2002) follow the trend of SD-MD magnetite (Fig. 8). FORC's data rather suggests a SD+SP assemblage (Fig. 9). Kfd measurements conducted on characteristic samples yielded no SP contribution and led to the conclusion that SP contribution is minor in our samples.

In conclusion, the magnetic mineralogy of the Portuguese CAMP is mainly controlled by fine Ti-poor titanomagnetite and accessorily maghemite and hematite depending on the oxidation state of the samples. Such mineralogy is typical of extrusive basalts of continental rifting (Dunlop and Özdemir, 1997) and we thus conclude that these rocks are good candidate for paleomagnetic studies.

6.2 Paleomagnetic reconstructions of Iberia at 200 Ma

Paleomagnetism is the unique geophysics tool that allows plate tectonic reconstruction for times older that ~180 Ma (i.e. the age of the oldest oceanic crust). It is based on the principle that inclination of the magnetization depends on the latitude of the plate (i.e. the so-called dipole law of the Geocentric Dipole Axial) and that the drift of a plate can be reconstructed by the drift of the corresponding paleomagnetic poles. Therefore, by comparing the paleomagnetic pole drift, called Apparent Polar Wander Path (APWP), of two distinct plates and at different times allow us to constrain the kinematic of plate tectonics. The best example is the opening of the Atlantic Ocean and the separation of Europe with North America (Fig. 12).

The problematic concerning the Iberian plate is that it's APWP its poorly constrained, notably for our interval of interest (Neres et al., 2012; Osete et al., 2011). Indeed, the unique high-quality paleomagnetic pole for Iberia at 200 Ma is the Messejana pole (Palencia-Ortas et al 2006; Osete et al., 2011) (Fig. 13).

When comparing our paleomagnetic poles with the APWP of Iberia computed from a compilation of Neres et al. (2012) and Osete et al. (2011), there is an overlap of the site-based mean pole with poles of younger age but the sample-based mean pole does not show any resemblance (Fig. 13). Anyhow, it is obvious that neither sample-based nor site-based paleomagnetic pole from this study show an overlap with the reference pole from the Messejana dyke (Palencia-Ortas et al., 2006). The partial resemblance with the poles from younger ages (70 Ma, 80 Ma, 180 Ma; Fig 12) is probably due to large a95 values of the site-based mean pole.

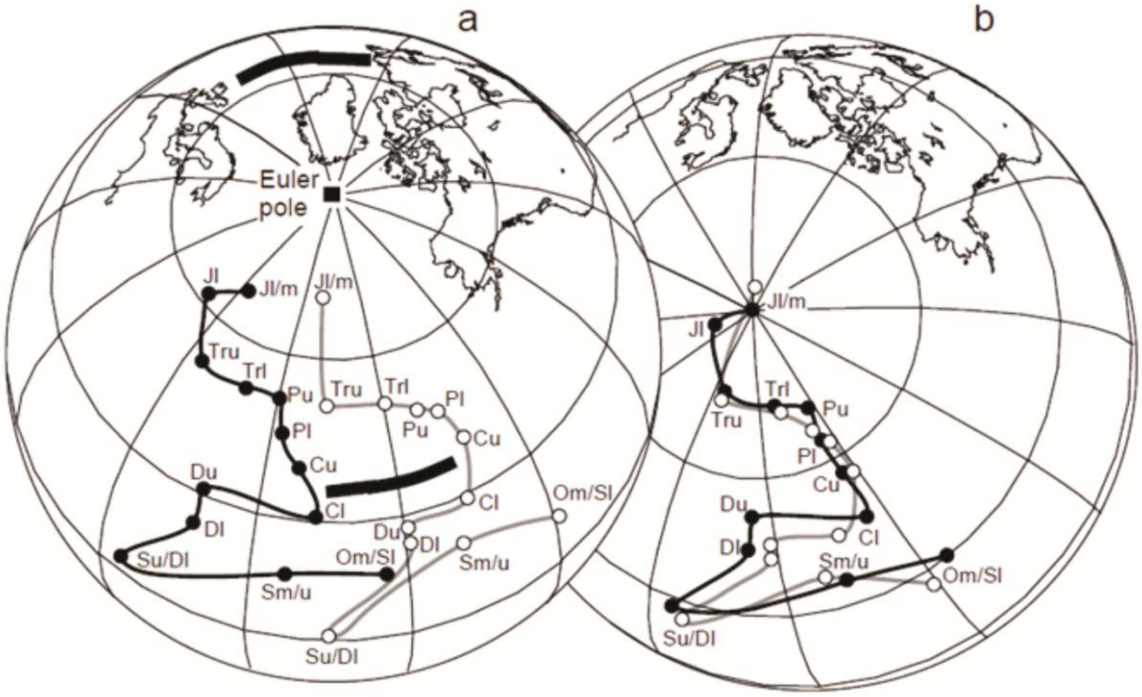

Figure 12:a) Paleozoic and Mesozoic APWP paths from North America (solid circles) and Europe (open circles). The solid square represents the Euler pole to reconstruct the APWP path of each plate; b) Middle Jurassic paleogeographic reconstruction of North America and Europe (c.f. Butler 1996).

By comparing our individual CAMP lava VGP's with individual VGP's from the Messejana dyke (Palencia-Ortas et al., 2006), we have found that this high dispersion is caused by the presence of two different VGP's distributions (Fig. 14). On one hand, there are four VGP's from this study (SB, QO, HT and JG) that fall within the Messejana VGP's distribution, whereas the remaining 4 VGP's (AL, AA, RL and FP; Fig. 14) are far from the mean direction of the first group and significantly distinct from Messejana VGP's distribution. Note that the difference between the two groups of directions resides essentially in changes in declination values and that VGP's from the B component directions are all geographically located at the central part of Algarve's basin (Fig. 1).

There are several hypotheses to explain the discrepancy between the directions of A and B components: Cretaceous remagnetization, different ages, lightning or tectonics. The Cretaceous remagnetization is excluded since there is no overlap between component B directions and the Cretaceous poles at 70 and 80 Ma (Fig. 13). The hypothesis of a different age for the component B is also unlikely because previous geochemical studies on Portuguese lava flows show a good agreement between the Moroccan basalts and the studied rocks, including local from component B (Marzoli et al., 2004). In addition, recent $^{40}Ar/^{39}Ar$ dating suggests that the lava flows from the Algarve basins are concordant with the $^{40}Ar/^{39}Ar$ ages of CAMP basalts from Moroccan basins (Verati et al., 2007). There is no significant difference between the age of the Alte lava outcrops (site AL here) and those from Santiago do Cacém and Tavira sites (Verati et al., 2007).

Lighting is a physical mechanism that can remagnetize superficial rocks. In such a case, the intensity of the NRM is thought to be more than one order higher than the original NRM intensity. In our case there is no significant increase in NRM intensities when comparing component A and component B data suggesting that lighting is not the favored hypothesis to explain the discrepancy between component A and B.

We rather suggest that significant tectonic movements on the central part of Algarve basin linked to complex movements on the São Marcos-Quarteira fault (SMQF) can produce significant deformations on the eastern part of the fault, accommodating various minor thrusts and folds (Terrinha, 1998). SMQF was reactivated during Mesozoic lithospheric extension and has been acting ever since.

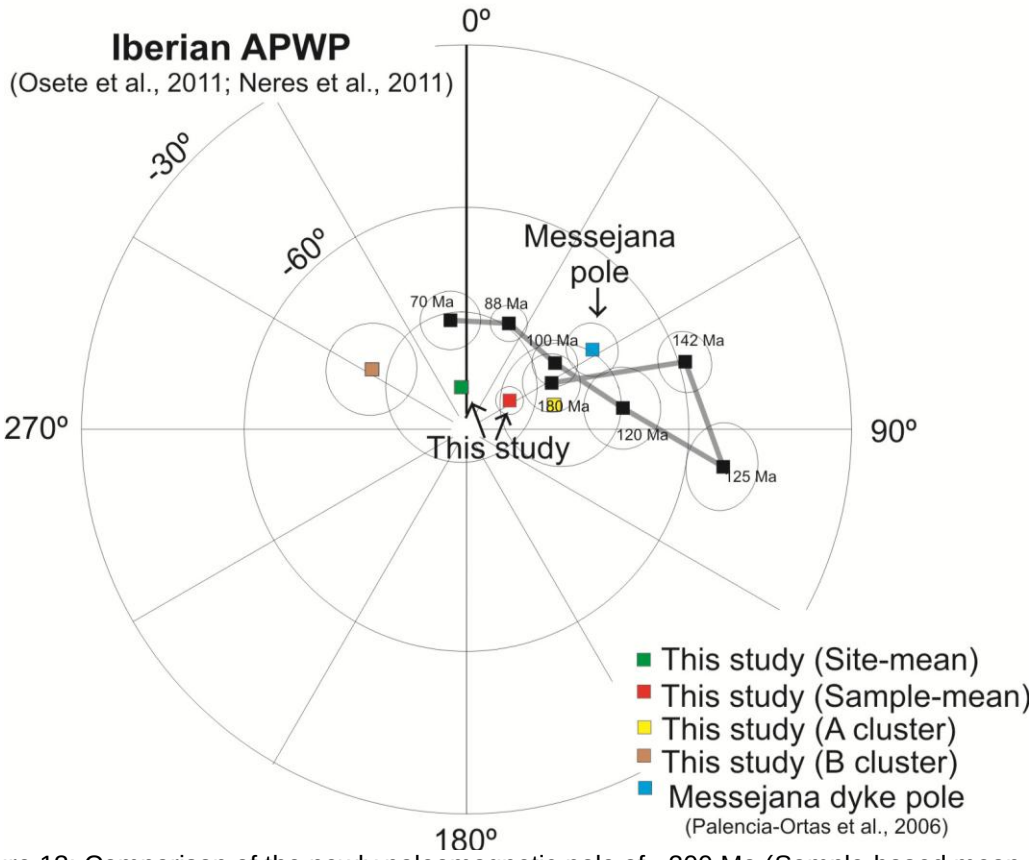

Figure 13: Comparison of the newly paleomagnetic pole of ~200 Ma (Sample-based mean, red square; Site-based mean, green square) with the APWP of the Iberian plate (Southern hemisphere represented) and with Messejana dyke pole (blue square). The mean “A component” and “B component” poles are also represented.

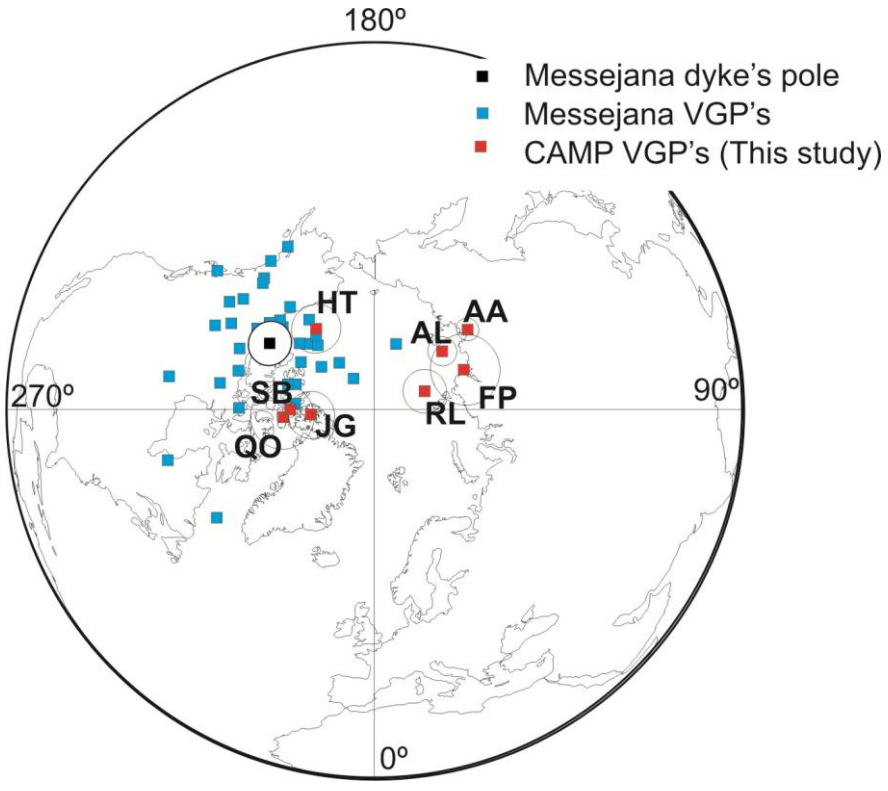

Figure 14: Comparison of the Portuguese CAMP VGP’s from this study with the Messejana VGP's.

6.3 Magnetostratigraphy of the Portuguese CAMP outcrops and its relationship with the Tr-J boundary

The link between the severe mass-extinction that took place at the Triassic- Jurassic boundary (~200 Ma) and the CAMP eruption is still very controversial. The problematic resides in the difficulty to date and correlate with accuracy the age of continental flood basalts from the CAMP lavas in continents and the age of the Triassic-Jurassic boundary in marine sections (Knight et al., 2004; Marzoli et al., 1999). In the Newark basin (USA), previous studies placed the Tr-J boundary before the eruptions of the first CAMP lavas (Kent and Olsen 1999) suggesting that CAMP cannot be responsible for the Tr-J crisis. According to the authors, the onset of CAMP volcanism is proposed to occur ~40 yr after the Tr-J boundary. On the other hand, based on geochemical data and $^{40}Ar/^{39}Ar$ dating of individual flows from Morocco and Newark, Marzoli et al. (2004) showed that the lowest unit basalts found in the Newark basin is correlated to the intermediate unit in the Moroccan basin. This means that the discrepancy between the Tr-J boundary and the first lavas found in both basin is due to the inexistence of the lower unit CAMP on the Newark basin.

Magnetostratigraphy has also been used to investigate the age and correlation of CAMP lavas from different continents. Magnetostratigraphic data of CAMP lavas from Newark basin and Moroccan basin encompasses a large interval of positive (normal) magnetic polarity, called the E24n chron. In Newark, Kent and Olsen (1999) identified a short interval of negative polarity located below the first CAMP lava and below the peak in spores interpreted by the authors to be the Tr-J boundary (Fig. 15). In Morocco, Knight et al. (2004) found a negative interval in the Intermediate unit of the Moroccan CAMP lavas, that the authors correlated to the E23r of Newark. Based on the presence of this reversal, Knight et al., (2004) suggested that the CAMP lavas in Morocco preceded the Tr-J boundary. However, these reversals were challenged by Font et al., (2011) who proved that they were result of chemical remagnetization. More recently Deenen et al. (2010) identified a negative shift in the C-isotope values just before the basalts deposition suggesting that the first Moroccan CAMP lavas coincide with the Tr-J mass extinction (Fig. 15).

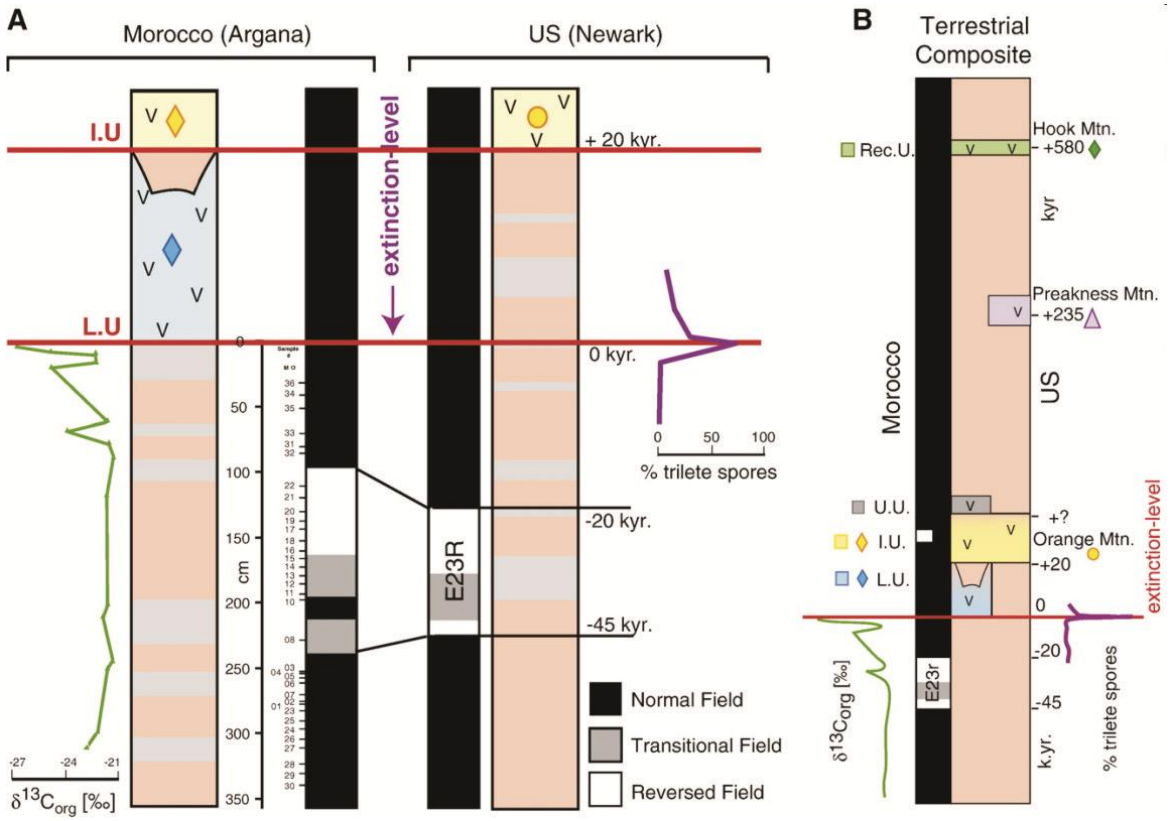

Figure 15: A) Trans- Atlantic CAMP correlation between Newark basin (US) and Argana basin (Morocco); B) Composite of the Terrestrial trans-Atlantic CAMP basins (c.f. Deenen et al., 2010).

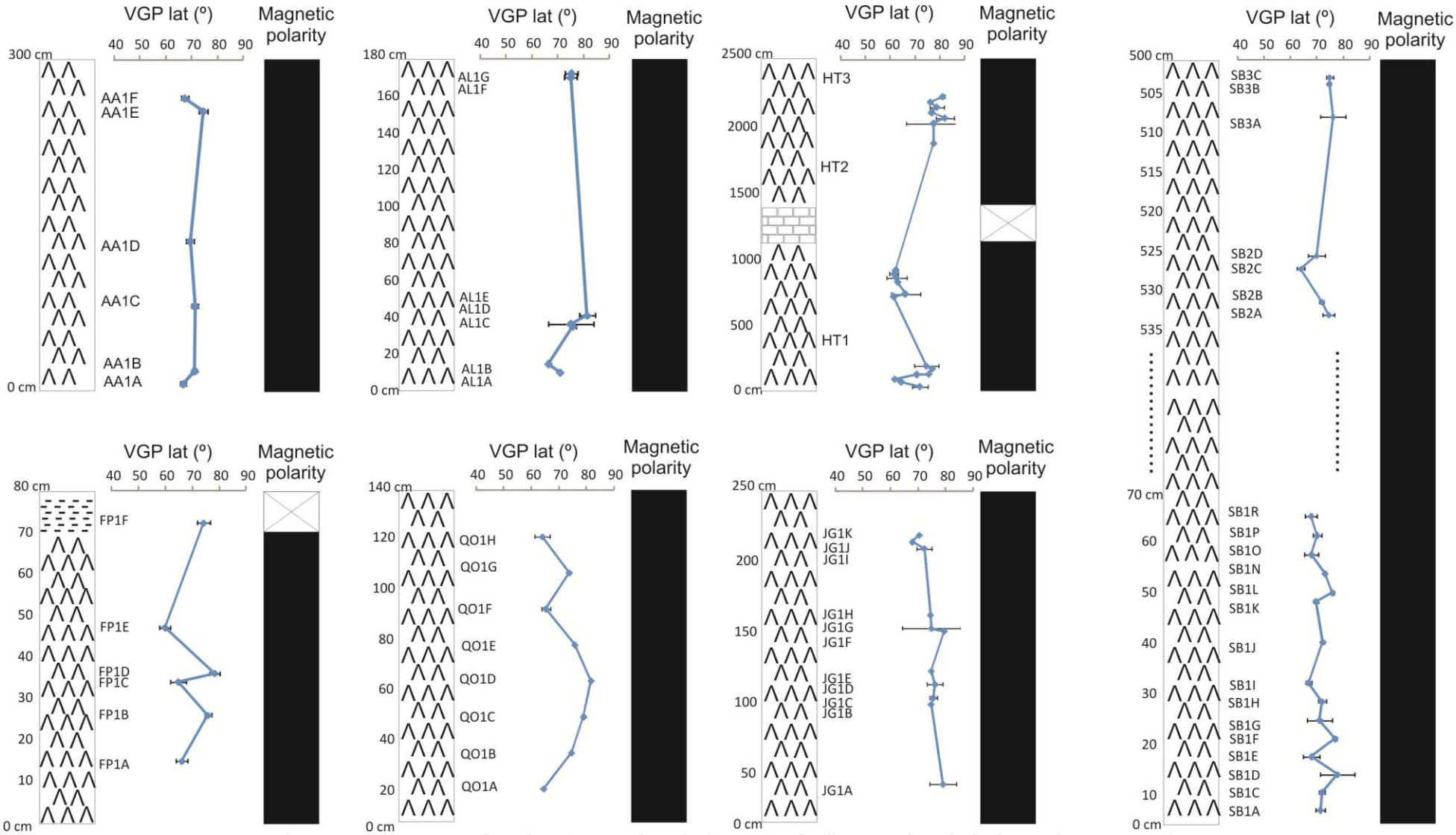

Figure 16: Magnetostratigraphy of CAMP basalts in Portugal. All magnetic polarity intervals are normal.

Here, we calculated a mean VGP for each individual flow (Fig. 16; Table A2). Seven sites with the corresponding VGP latitude variations are displayed (Fig. 16). All samples collected in the Algarve basin display a positive (normal) remanent magnetization, confirming previous magnetostratigraphic studies conducted on CAMP's lavas worldwide (Kent et al., 1999; Deenen et al., 2011; Font et al., 2011). Considering that recent radio-isotopic ages have been conducted on Algarve's outcrops and yielded a mean age of 198.1±0.4 Ma, (Verati et al., 2007) the positive interval found in all paleomagnetic sites is here correlated to the E24n Superchron (Fig. 15). No reverse anomaly has been found contrarily to Knight et al. (2004).

Comparing the paleomagnetic (Dec and Inc) directions of successive lava flows also provide information about eruptions times (Chenet et al., 2009). In this study, we found no significant variations of paleomagnetic direction per site except for HT site that has two distinct volcanic pulses separated by a thin interval of dolomite (Fig. 16; Table A2). The remaining sites don't display significant variations on paleomagnetic directions which led us to the conclusion that a single volcanic pulse is present.

7. Conclusion

The main findings of this study may be summarized as follows:

1. Magnetic mineralogy indicates that the main magnetic carriers are primary Ti-poor titanomagnetite with accessorily presence of maghemite and hematite in some samples. Such mineralogy is typical of continental basalt and indicates that these rocks are good candidates for paleomagnetic study.
2. AF cleaning provided stable demagnetization patters at high field which yielded normal polarities ChRM (Tilt corrected) located at: Dec=0º; Inc=52.8º; a95=9.8º, N=8. The corresponding pole is located at: Plat=84.4º, Plong=177.9º (K= 32.9; A95=9.8º)
3. The lack of consistency of this pole with those obtained by Palencia-Ortas et al., (2006) is probably due to the existence of two different VGP's distributions (component A and component B) that shifts the pole direction away from the Messejana pole. Component A shares the same distribution as the Messejana VGP's, whereas component B does not share the same distribution.
4. The origin of the discrepancy between component A and component B is attributed to tectonic movements on the central region of the Algarve basin.
5. All Portuguese CAMP lavas encompass a normal magnetic polarity interval and no negative interval has been depicted. It confirms previous results by Font et al. (2011) that the E23r anomaly of the Newark basin is not recorded in the Moroccan and Portuguese CAMP lava flows. The normal polarity is correlated to the E24n chron.
6. Short variations in VGP latitudes and longitude along individual lava flows suggests a relatively rapid cooling time. Except for the outcrops located near Sagres (HT) where two distinct pulses are separated by a thin (~1-2 m) interval of dolomite, most of the studied sections represent a single volcanic pulse.

8. Appendices

Table A1: Kfd measurements. klf is the lower magnetic field (976 Hz), khf is the higher magnetic field applied (15616 Hz), kfd is ratio (khf-k1f)/k1f.

Sample	K1f	Khf	Kfd	Kfd(%)
FP1A1	1.76E-02	1.75E-02	6.99E-03	0.70
FP1B2	1.52E-02	1.51E-02	6.37E-03	0.64
FP1C4	9.55E-03	9.48E-03	7.62E-03	0.76
FP1D3	1.37E-02	1.36E-02	5.86E-03	0.59
FP1E3	1.81E-02	1.80E-02	7.13E-03	0.71
FP1F1	1.99E-02	1.98E-02	6.14E-03	0.61
AL1A2	1.61E-02	1.60E-02	7.74E-03	0.77
ALB1	2.84E-02	2.82E-02	6.65E-03	0.67
AL1C2	2.47E-02	2.45E-02	7.94E-03	0.79
AL1D2	2.54E-02	2.52E-02	6.90E-03	0.69
AL1E1	2.60E-02	2.58E-02	6.27E-03	0.63
AL1F1	2.77E-02	2.75E-02	5.74E-03	0.57
AL1G2	2.21E-02	2.19E-02	5.94E-03	0.59
AL1H3	2.07E-02	2.06E-02	7.01E-03	0.70
SB1A5	1.08E-02	1.07E-02	1.13E-02	1.13
SB1C2	1.13E-02	1.11E-02	1.32E-02	1.32
SB1D1	1.27E-02	1.25E-02	1.21E-02	1.21
SB1G3	1.31E-02	1.30E-02	9.66E-03	0.97
SB2A1	1.61E-02	1.59E-02	9.51E-03	0.95
SB2B2	1.85E-02	1.83E-02	9.36E-03	0.94
SB2C2	1.50E-02	1.48E-02	1.05E-02	1.05
SB2D1	1.20E-02	1.19E-02	1.06E-02	1.06
SB3A2	1.62E-02	1.60E-02	9.03E-03	0.90
SB3B1	1.76E-02	1.75E-02	9.30E-03	0.93
SB3C2	1.65E-02	1.64E-02	9.09E-03	0.91
SB4A1	1.03E-02	1.01E-02	1.71E-02	1.71
SB4B4	1.00E-02	9.88E-03	1.60E-02	1.60
SB4C2	1.12E-02	1.10E-02	1.54E-02	1.54
SB4D3	1.18E-02	1.16E-02	1.46E-02	1.46

Table A2: Mean ChRM per flow of each paleomagnetic pole

Mean ChRM per flow

Site	Dec	Inc	N	k	a95
AA1A	19.3	36.5	3	4052.5	1.9
AA1B	7.9	36.5	5	2516.8	1.5
AA1C	11	36.7	5	1097.4	2.3
AA1D	14.9	37	4	832.3	3.2
AA1E	13.6	44.3	4	742	3.4
AA1F	20.3	38.9	5	677.4	2.9
AL1B	12.7	37.9	1	0	0
AL1C	19.5	36.8	1	0	0
AL1D	11.3	44.9	3	2654.6	2.4
AL1E	12.7	44.8	2	203.1	17.6
AL1F	6	49	4	218.2	6.2
AL1G	8.3	41.4	5	223.7	5.1
AL1H	13.4	46.1	4	363.7	4.8
AY1A	76.7	81	2	0.3	
AY1B	33.4	77.6	2	1268.7	7
AYC	120.7	86.6	2	47127	1.2
AY1C	120.7	86.6	2	47127	1.2
AY1D	19.8	86.2	2	269.6	15.3
AY1G	347.2	56.5	1	0	0
AY1I	55.1	35.5	1	0	0
AY1J	54.4	75.1	1	0	0
AY1K	59.3	58.4	1	0	0
AY2A	12.3	73.2	2	28.4	48.8
AY2B	1.8	67.5	3	13.4	35
AY2C	345.1	68	2	685.2	9.6
AY2D	33.6	76.2	1	0	0
FP1A	27.3	51.1	3	588.3	5.1
FP1B	10.2	47.8	3	1730.3	3
FP1C	27.2	46.8	4	177.5	6.9
FP1D	3.2	47.7	3	741.9	4.5
FP1E	32	41.9	4	389.4	4.7
FP1F	354.8	41.9	5	190.8	5.6
HT1A	358	36.8	2	1171.8	7.3
HT1B	8.1	23.9	1	0	0
HT1C	339.1	28.6	1	0	0
HT1D	355.7	35.1	1	0	0
HT1D	355.7	35.1	1	0	0
HT1E	4.2	43.2	1	0	0
HT1F	359.5	44.8	1	0	0
HT1G	353.7	42.5	2	446.7	11.8
HT2A	332.1	37.7	1	0	0
HT2B	334.2	46.6	2	334.6	13.7
HT2C	338.5	32.4	1	0	0
HT2D	335.2	35.6	2	632.3	9.9
HT2E	333.7	34.8	2	3679.2	4.1
HT2F	333.8	37	2	40920	1.2
HT3A	348.9	52	1	0	0
HT3B	352.8	47.8	2	94.8	25.9
HT3C	354.3	54.9	2	817	8.7
HT3D	0.1	44.2	1	0	0
HT3E	355.6	48.2	2	1442.3	6.6
HT3F	349	48.8	1	0	0
HT3G	353.8	53.5	2	19784.5	1.8
JG1A	355.6	62.3	2	489.5	11.3
JG1B	344.6	58.3	1	0	0
JG1C	347	52.8	2	5645.1	3.3
JG1D	346.8	59	3	360.4	6.5
JG1E	348.4	64	1	0	0
JG1F	2.9	62.2	1	0	0
JG1G	347.4	50.3	2	103.1	24.8

Mean ChRM per flow

Site	Dec	Inc	N	k	a95
QOB	337.1	38.9	1	0	0
QOC	344.8	62.5	2	25266.9	1.6
QOD	349.6	56.1	1	0	0
QOE	353.7	56	1	0	0
QOF	345.7	60.8	2	4810	3.6
QOG	330.8	53.1	1	0	0
QOH	342.1	59.1	2	1582.2	6.3
QOI	327.5	63.5	1	0	0
RL1A	17.6	59	1	0	0
RL1B	12.5	51.6	1	0	0
RL1C	9.6	51.7	1	0	0
RL1D	188.3	72.9	1	0	0
RL1E	12.3	53.9	1	0	0
RL1F	7.1	50.3	1	0	0
RL1G	14.8	51.3	1	0	0
RL1H	9.7	46.8	1	0	0
RL1I	6.9	46.3	1	0	0
RL2A	8.4	55.7	1	0	0
RL2B	4.2	51.7	1	0	0
RL2C	348.7	52.3	1	0	0
RL2F	11.8	54.2	1	0	0
RL2G	13.2	51.3	1	0	0
SB1A	339.8	56.8	5	326.4	4.2
SB1C	340.6	57.8	4	1296.8	2.6
SB1D	349.7	56.8	3	61.4	15.9
SB1E	334.9	55.6	4	141.6	7.7
SB1F	348.4	56.3	3	4920	1.8
SB1G	345.1	59.3	2	203.8	17.6
SB1G	339.2	58	3	134.5	10.7
SB1H	340.8	57.2	4	589.5	3.8
SB1I	333.6	54.4	4	1111.3	2.8
SB1J	341.1	57.8	4	3210.7	1.6
SB1K	337.2	57	4	1845.5	2.1
SB1L	349.1	62.4	3	8192	1.4
SB1N	343	61	4	9884.5	0.9
SB1O	334.7	62.1	2	1697.4	6.1
SB1P	337.9	58.1	4	536.5	4
SB1R	335.4	53.6	3	548.6	5.3
SB2A	349.2	51.6	5	232.8	5
SB2B	344.1	51.3	2	10192.7	2.5
SB2C	329.2	51.4	3	767.2	4.5
SB2D	340.6	50.7	3	180.5	9.2
SB3A	350.5	59.2	2	319	14
SB3B	347.5	56.2	5	1432.5	2
SB3C	347.8	58.9	3	978.8	3.9
SB4B	352.6	59.7	5	942.4	2.5
SB4C	353.7	60.8	4	5165.4	1.3
SB4D	343.3	59.8	2	3059.3	4.5
SB1E	349.1	59.5	5	1753.5	1.8
SB4E	349.1	59.5	5	1753.5	1.8
SB4F	352.4	55.7	4	592.8	3.8
SB1G	343.5	57.3	4	543.1	3.9
SB4H	343.2	56.8	4	403	4.6
SB4I	342.1	55.2	2	6163.6	3.2

9. References

Besse, J. and Courtillot V., 2002. Apparent and true polar wander and the geometry of the geomagnetic field over the last 200 Myr. Journal of Geophysical Research, 107: 1-31.

Butler R.F., 1996. Paleomagnetism: Magnetic Domains to Geologic Terranes. Electronic Edition.

Chenet A.L, Fluteau F., Courtillot V., Gerard M. and Subbarao K. V., 2006. Determination of rapid Deccan eruptions across the Cretaceous-Tertiary boundary using paleomagnetic secular variation: Results from a 1200-m-thick section in the Mahabaleshwar escarpment. Journal of Geophysical Research, 113: 1-27.

Day R., Fuller M. and Schmidt V.A., 1977. Hysteresis properties of titanomagnetites: Grain size and compositional dependence. Physics of the Earth and Planetary Interiors, 13: 260-267.

Dearing J., 1994. Environmental Magnetic Susceptibility

Deenen M. H. L., Langereis C. G., van Hinsbergen D. J. J. and Biggin A.J., 2011. Geomagnetic secular variation and the statistics of palaeomagnetic directions. Geophysical J. Int: 1-12.

Deenen M.H.L. et al., 2010. A new chronology for the end-Triassic mass extinction. Earth and Planetary Science Letters: 1-13.

Dunlop D.J., 2002 a. Theory and application of the Day plot (Mrs/Ms versus Hcr/Hc) 1. Theoretical curves and tests using titanomagnetite data. Journal of Geophysical Research, 107: 1-22.

Dunlop D.J., 2002 b. Theory and application of the Day plot (Mrs/Ms versus Hcr/Hc) 2. Application to data for rocks, sediments, and soils. Journal of Geophysical Research, 107: 1-15.

Dunlop D.J. and Özdemir O., 1997. Rock Magnetism: Fundamentals and frontiers.

Fisher R., 1953. Dispersion on a sphere. Proc. R. Soc. A., 217: 295-305.

Font E. et al., 2011. Revising the magnetostratigraphy of the Central Atlantic Magmatic Province (CAMP) in Morocco. Earth and Planetary Science Letters: 1-16.

Hrouda F., 2002. Variations in magnetic anisotropy and opaque mineralogy along a kilometer deep profile within a vertical dyke of the syenogranite porphyry at CÍnovec (Czech Republic). Journal of Volcanology and Geothermal Research, 113: 37-47.

Hrouda F., 2003. Indices for numerical characterization of the alteration process of magnetic minerals taking place during investigation of temperature variation of magnetic susceptibility. Stud. Geophys. Geod.,, 47: 847-861.

Kent D.V. and Olsen P.E., 1999. Astronomically tuned geomagnetic polarity timescale for the Late Triassic. Journal of Geophysical Research, 104: 831-841.

Kirschvink J. L., 1980. The least-squares line and plane and the analysis of paleomagnetic data. Gepphys. J. R. Astron. Soc., 62: 699-718.

Knight K.B. et al., 2004. The Central Atlantic Magmatic Province at the Triassic-Jurassic boundary: paleomagnetic and (40)Ar/(39)Ar evidence from Morocco for brief, episodic volcanism. Earth and Planetary Science Letters, 228: 143-160.

Kruiver P., Dekkers M.J. and Heslop D., 2001. Quantification of magnetic coercivity components by the analysis of acquisition curves of isothermal remanent magnetization. Earth and Planetary Science Letters, 189: 269-276.

Labails C., Olivet J.L., Aslanian D. and Roest W.R., 2010. An alternative early opening scenario for the Central Atlantic Ocean. Earth and Planetary Science Letters, 297: 355-368.

Lowrie W., 1997. Fundamentals of Geophysics. Cambridge University Press.

Martínez V.C., Torsvik T.H., Van Hinsbergen D.J.J. and Gaina C., 2012. Earth at 200 Ma: Global palaeogeography refined from CAMP paleomagnetic data. Earth and Planetary Science Letters, 331-332: 67-79.

Martins L.T. et al., 2008. Rift-related magmatism of the Central Atlantic magmatic province in Algarve, South Portugal. LITHOS, 101: 102-124.

Marzoli A. et al., 2004. Synchrony of the Central Atlantic magmatic province and the Triassic-Jurassic boundary climatic and biotic crisis. Geology, 32: 973-976.

Marzoli A. et al., 1999. Extensive 200-Million-Year-Old Continental Flood Basalts of the Central Atlantic Magmatic Province. Science, 284: 616-618.

McFadden P.L. and Lowes F.J., 1981. The discrimination of mean directions drawn from Fisher distributions. Geophysic. J. R., 67: 19-33.

McFadden P.L. and McElhinny M.W., 1999. Paleomagnetism: Continents and Oceans. Academic Press.

McHone J.G., 2002. Volatile Emissions from Central Atlantic Magmatic Province Basalts: Mass Assumptions and Environmental Consequences. Geophysical Monograph: 1-11.

Muxworthy A.R. and Dunlop D.J., 2002. First-order reversal curve (FORC) diagrams for pseudo-single-domain magnetites at high temperature. Earth and Planetary Science Letters, 203: 369-382.

Neres M. et al., 2012. Reconciling Cretaceous paleomagnetic and marine magnetic data for Iberia: New Iberian paleomagnetic poles. J. Geophys.Res., 117: 1-21.

Olivet J.L., 1996. Kinematics of the Iberian plate. Bull. Centres Rech. Explor. Elf Aquitaine, 20: 131-195.

Osete M.L. et al., 2011. The evolution of Iberia during the Jurassic from paleomagnetic data. Tectonophysics, 502: 105-120.

Özdemir, Ö., 1987. Inversion of titanomaghemites. Earth and planetary Interiors, 46: 184-196.

Özdemir, Ö., Dunlop, D.J. and Moskowitz, B.M., 1993. The effect of oxidation on the Verwey transition in magnetite. Geophys. Res. Lett.,, 20: 1671-1674.

Palencia Ortas A., Osete M.L., Vegas R. and Silva P., 2006. Paleomagnetic study of the Messejana Plasencia dyke (Portugal and Spain): A lower Jurassic paleopole for the Iberian plate. Tectonophysics, 420: 455-472.

Pálfy J., 2003. Volcanism of the Central Atlantic Magmatic Province as a Potential Driving Force in the End-Triassic Mass Extintion. Geophysical Monograph, 136: 255-264.

Petrovsky E. and Kapricka A., 2006. On determination of the Curie point from thermomagnetic curves. Journal of Geophysical Research, 111: 1-10.

Rapaille C. et al., 2002. Geochemistry and age of the European CAMP basalts.

Roberts A. P., 2000. First-order reversal curve diagrams: A new tool for characterizing the magnetic properties of natural samples. Journal of Geophysical Research, 105: 28,461-28,475.

Robertson D.J. and France D.E., 1994. Discrimination of remanence-carrying minerals in mixtures, using isothermal remanent magnetization acquisition curves. Physics of the Earth and Planetary Interiors, 82: 223-234.

Terrinha P., 1998. Structural Geology and Tectonic Evolution of the Algarve Basin, South Portugal.

Torsvick T.H., Dietmar Müller R., Van Der Voo R., Steinberger B. and Gaina C., 2008. Global plate motion frames: Toward a unified model. Reviews of Geophysics, 46: 1-44.

Torsvick T.H. et al., 2012. Phanerozoic Polar Wander, Palaeogeography and Dynamics. Earth-Science Reviews: 1-138.

Van Der Voo R., 1990. The reliability of paleomagnetic data. Tectonophysics, 184: 1-9.

Vandamme D., 1994. A new method to determine paleosecular variation. Physics of the Earth and Planetary Interiors, 85: 131-142.

Verati C. et al., 2007. (40)Ar/(39)Ar ages and duration of the Central Atlantic Magmatic Province volcanism in Morocco and Portugal and its relation to the Triassic-Jurassic boundary. Palaeogeogr. Palaeoclimatol. Palaeoecol., 244: 308-325.

Vissers P.Th. and Meijer R.L.M., 2012. Iberian plate kcinematics and Alpine collision in the Pyrenees. Earth-Science Reviews, 114: 61-83.

Youbi N. et al., 2003. The Late Triassic-Early Jurassic Volcanism of Morocco and Portugal in the Framework of the Central Atlantic Magmatic Province: an Overview. Geophysical Monograph, 136: 179-207.